

This is the author's manuscript for publication. The publisher-formatted version may be available through the publisher's web site or your institution's library.

Dynamic factor analysis of surface water management impacts on soil and bedrock water contents in Southern Florida Lowlands

I. Kisekka, K. W. Migliaccio, R. Muñoz-Carpena, B. Schaffer, Y. C. Li

How to cite this manuscript

If you make reference to this version of the manuscript, use the following information:

Kisekka, I., Migliaccio, K. W., Muñoz-Carpena, R., Schaffer, B., & Li, Y. C. (2013). Dynamic factor analysis of surface water management impacts on soil and bedrock water contents in Southern Florida Lowlands. Retrieved from <http://krex.ksu.edu>

Published Version Information

Citation: Kisekka, I., Migliaccio, K. W., Muñoz-Carpena, R., Schaffer, B., & Li, Y. C. (2013). Dynamic factor analysis of surface water management impacts on soil and bedrock water contents in Southern Florida Lowlands. *Journal of Hydrology*, 488, 55-72.

Copyright: © 2013 Elsevier B.V.

Digital Object Identifier (DOI): doi:10.1016/j.jhydrol.2013.02.035

Publisher's Link: <http://www.sciencedirect.com/science/article/pii/S0022169413001583>

This item was retrieved from the K-State Research Exchange (K-REx), the institutional repository of Kansas State University. K-REx is available at <http://krex.ksu.edu>

27 contents in terms of regression coefficient magnitude was canal stage. Based on DFA results, a simple
28 regression model was developed to predict soil and bedrock water contents at various elevations as a
29 function of canal stage and net recharge. The performance of the simple model ranged from good (C_{eff}
30 ranging from 0.56 to 0.74) to poor (C_{eff} ranging from 0.10 to 0.15), performance was better at sites with
31 smaller depths to water table (< 1 m) highlighting the effect of micro-topography on soil and bedrock
32 water content dynamics. Assessment of the effect of 6, 9 and 12 cm increases in canal stage using the
33 simple regression model indicated that changes in temporal variation in soil and bedrock water contents
34 were negligible (average $< 1.0\%$ average change) at 500 to 2000 m from C111 (or low elevations) which
35 may be attributed to the near saturation conditions already occurring at these sites. This study used DFA
36 to explore the relationship between soil and bedrock water dynamics and surface water stage in shallow
37 water table environments. This approach can be applied to any system in which detailed physical
38 modeling would be limited by inadequate information on parameters or processes governing the physical
39 system.

40 **Key words:** Soil water content, bedrock water content, scaled frequency, Dynamic Factor Analysis, canal
41 stage, water table

42 Abbreviations: DFA, dynamic factor analysis; SF, scaled frequency; R_{net} , net surface recharge; MWT,
43 mean water table elevation; S177T, C111 canal stage; SFWMD, South Florida Water Management
44 District; AIC, Akaike information criterion; BIC, Bayesian information criterion; VIF, variance inflation
45 factor; NGVD29, National Geodetic Vertical Datum of 1929.

46

47 **1. Introduction**

48 In an attempt to correct some of the undesired consequences of south Florida's extensive drainage
49 canal network on the region's ecosystem, an environmental restoration project named the Comprehensive
50 Everglades Restoration Plan (CERP) is currently under implementation. CERP was approved by the
51 United States Congress under the Water Resources Development Act (2000). One of the 68 components
52 that comprise CERP is the C111 spreader canal project whose goal is to reduce the impacts of C111 (i.e.,
53 reduce groundwater seepage into C111) on Everglades National Park (ENP) and Taylor Slough which is a
54 natural drainage feature that conveys water to Florida while maintaining existing levels of flood
55 protection in the adjacent agricultural and urban areas (U.S. Army Corps of Engineers [USACP] and
56 South Florida Water Management District [SFWMD], 2009). As part of the C111 spreader canal project,
57 structural modifications and operational adjustments involving incremental raises in canal stage are
58 planned along one of the major canals (i.e., C111) separating ENP and agricultural production areas to the
59 east of the canal. The increase in canal stage will occur by changing surface water management at the
60 gated spillway located at structure named S18C (Fig. 1) in the form of incremental raises in canal stage of
61 up to 12 cm.

62 It is anticipated that the planned rise in C111 canal stage will affect water table levels in the adjacent
63 agricultural areas. Earlier research indicated that there is substantial interaction between the highly
64 permeable Biscayne aquifer and water level in canals (Genereux and Slater, 1999). The hydraulic
65 connection between Biscayne aquifer and canal C111 causes the shallow water table system to fluctuate
66 with respect to changes in canal stage. Using the drain to equilibrium assumption, Barquin et al. (2011)
67 showed that water table elevation in the Biscayne aquifer significantly influenced soil and bedrock water
68 contents in a fruit orchard with soil and bedrock formations that are very similar to our current study site.
69 Therefore, raising water table elevation could result in increased soil and bedrock water contents or
70 greater saturation of the root zone which could affect the production of winter vegetables predominately
71 grown in this area. Saturation of the root zone could impact yield potential by impairing root growth due

72 to anoxia, reducing stomatal conductance, and reducing net CO₂ assimilation (Schaffer, 1998). In addition
73 to physiological stress, having the soils saturated could render movement of machinery difficult and also
74 impact growing season and market dates. However, it is not known to what extent the proposed structural
75 modifications and operational adjustments along canal C111 would impact water table elevations and thus
76 soil and bedrock water contents in agricultural areas east of the canal.

77 Vegetable production in Miami-Dade County, a substantial proportion of which is located along the
78 extensive eastern boundary of ENP, is a significant contributor to both the local and state economies.
79 According to the 2007 Census of Agriculture from the US Department of Agriculture (USDA, 2007), the
80 total value of vegetables produced in Miami-Dade County was over 128 million dollars in 2007. Green
81 beans, sweet corn, squash, tomatoes and sweet potato are the dominant vegetables grown in the area.
82 There is need to quantify the impacts of hydrological modifications and surface water management on
83 agricultural land use at field scale because large regional hydrology models have discretization that might
84 not be suitable for resolving small scale micro-topographic differences within the landscape.

85 Long term monitoring and exploratory analysis of soil and limestone bedrock water contents could
86 characterize the effect of various drivers on the temporal variability of water contents. The soils in the
87 agricultural areas east of C111 were created from scarification of the underlying limestone bedrock hence
88 they are very shallow and have high gravel content. Three main stresses that influence soil water content
89 that could be included in exploratory analysis are 1) canal stage, which affects water table elevation; 2)
90 rainfall, and 3) evapotranspiration. While these stresses may be assessed using physically based models of
91 vadose zone flow and transport, implementation of unsaturated flow models (e.g., WAVE [Vanclooster
92 et al., 1995] or HYDRUS [Šimůnek, et al., 2008]) is not an easy task since they contain numerous
93 parameters and processes that have to be quantified (Ritter et al., 2009). In very gravelly and shallow soils
94 such as those in south Miami-Dade County, quantifying parameters such as hydraulic conductivity for use
95 in Richards' equation is further complicated by having porous gravelly soils that are not homogeneous.
96 Previous applications of WAVE, for example, in gravelly soils of south Florida have indicated that a

97 detailed description of soil hydraulic properties (e.g., using dual porosity) could result in improved
98 robustness of vadose zone models (Duwig et al., 2003; Muñoz-Carpena et al., 2008). Therefore the
99 success of applying physically based models to simulate soil and bedrock water dynamics depends largely
100 on proper conceptualization of location specific processes and proper measurement or estimation of
101 parameters. In this context, complementary exploratory tools such as Dynamic Factor Analysis (DFA)
102 which are not processes based are desired as simpler preliminary exploratory tools that could also be used
103 for preliminary predictions of the impact of surface water management decisions on land use.

104 A comprehensive description of DFA and modeling can be found in Zuur et al. (2003). For purposes
105 of aiding discussion, we only provide a brief description of this technique. DFA is a dimension reduction
106 multivariate time series analysis technique that is used to estimate underlying common patterns (common
107 trends) in short time series as well as the effect of explanatory variables on response variables. The
108 advantage of DFA over other traditional dimensional reduction techniques (e.g., Factor Analysis or
109 Principal Component Analysis) is that DFA accounts for the time component. This allows the underlying
110 hidden effects driving the temporal variation in the observed time series data to be detected (Zuur et al.,
111 2003). DFA does not require observed time series to be long and stationary. Although non-stationarity
112 could be handled through de-trending, trends in the times series could hold necessary information
113 required to explain the temporal dynamics in the observed variable (Ritter et al., 2009). In addition, DFA
114 can handle missing values in the observed time series (i.e., DFA does not require data sets to be regularly
115 spaced). Missing values in observed time series data sets are not uncommon especially when time series
116 data are obtained from unattended automatic data logging field instruments (e.g., multi-sensor capacitance
117 probes for soil water monitoring).

118 DFA applications are documented in literature from several disciplines (e.g., Geweke, 1977; Márkus
119 et al., 1999; Zou and Yu, 1999; Zuur et al., 2003; Zuur and Pierce, 2004; Muñoz-Carpena et al., 2005;
120 Ritter and Muñoz-Carpena, 2006; Zuur et al., 2007; Ritter et al., 2009; Kaplan et al., 2010a; Kaplan and
121 Muñoz-Carpena, 2011). Thus, we only provide a brief review of the most relevant examples. Ritter and

122 Muñoz-Carpena (2006) applied DFA and modeling to study interactions between surface water and
123 groundwater levels within the Frog Pond agricultural area located west of canal C111 in south Florida
124 (Fig.1). Their results indicated that the two canals surrounding the Frog Pond area had the greatest
125 influence on temporal changes in water table elevation. Their study did not address the issue of the impact
126 of surface management decisions on soil water content. Soil water is a major concern for vegetable
127 growers in south Florida due to the impact saturated or near saturated soil conditions have on planting
128 dates and yield losses (Fig. 1).

129 Others have applied DFA and modeling to study soil water dynamics. Ritter et al. (2009) applied
130 DFA to analyze temporal changes in soil water status of a humid, subtropical, evergreen forest in Canary
131 Islands, Spain. Kaplan and Muñoz-Carpena (2011) applied DFA to study the complementary effects of
132 surface and groundwater on soil water dynamics in a coastal flood plain. Thus, DFA was successfully
133 used to identify unexplained variability in observed hydrologic time series and to assess the effect of
134 selected explanatory variables on response variables (observed time series of interest).

135 The difference between our study and prior studies is that we applied DFA to investigate the effect of
136 surface water management in canals on soil water dynamics in an agricultural area with very shallow very
137 gravely loam soils, and unlike in the previous studies we also considered not only the effects of potential
138 evaporation (ET_0) but also the effect of water table evaporation given the shallow water table. We then
139 attempted to develop a simple model, using information from the DFA, to predict soil water content from
140 easily measured variables such as canal stage and recharge (i.e., difference between rainfall and
141 evapotranspiration). Canal stage was selected instead of water table elevation since water table elevation
142 data in our study area are less complete due to the limited period of record and the limited number of
143 continuously monitored groundwater wells. Canal stage has been monitored for a longer period of record
144 and has no foreseeable end of data collection, thus it is a more reliable measurement for long-term use.
145 We assumed that at any given time, water table elevation is approximately equal to canal stage. We
146 concede that at certain times this assumption might not hold e.g., immediately after or during storm

147 events; however, due to the high permeability of the aquifer and the daily time step used, the assumption
148 holds for the majority of the time.

149 The goal of this study was to use DFA and modeling to investigate how the proposed raises in canal
150 stage along C111 could impact soil and bedrock water contents in low lying farmlands located between
151 canals C-111 and C-111E. The specific objectives were to: (1) apply DFA to identify the most important
152 factors affecting temporal variation in soil and bedrock water contents, (2) develop a simplified DFA
153 based regression model for predicting soil and bedrock water contents as a function of canal stage, and (3)
154 use the developed simple regression model to predict the impact of proposed incremental raises in canal
155 stage on soil and bedrock water contents at various elevations and distances from the canal.

156 **2. Materials and methods**

157 **2.1 Experimental site**

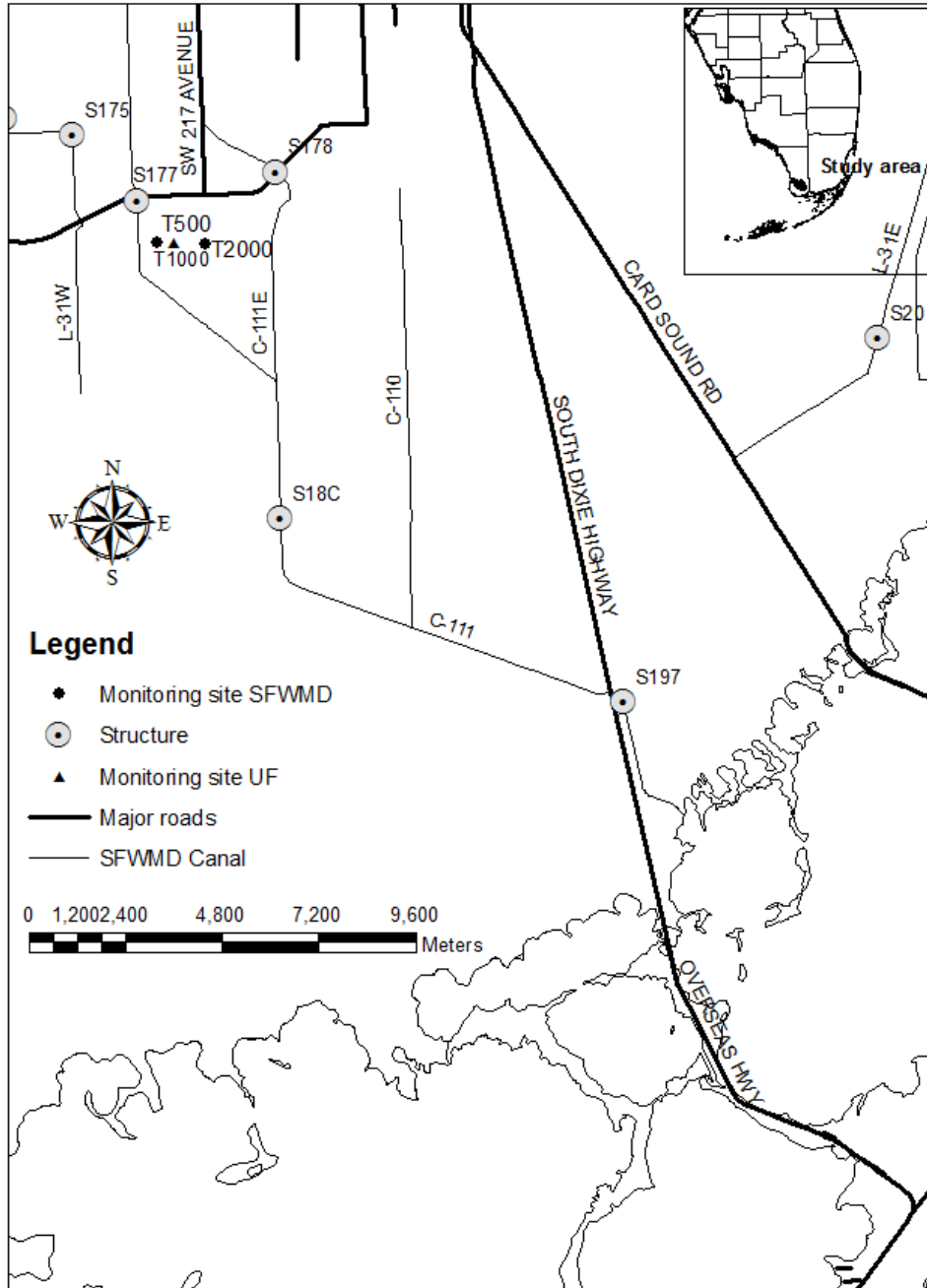
158 The study was conducted in southern Miami-Dade County, Homestead, Florida, United States in a
159 small agricultural area approximately 17 km² (Fig. 1). The area is located east of ENP between SFWMD
160 canals C111 and C111E which are planned to experience increases in canal stage under the C111 spreader
161 canal project. Canal stage upstream in the two canals is controlled by a remotely operated spillway at
162 S177 and a culvert at S178, respectively (Fig. 1). C111 is the larger of the two canals and the two join to
163 become a single canal at the southern end of the study area which is managed using a gated spillway at
164 S18C. It is proposed that stage will be increased by modifying operation of S18C and thus affect canal
165 stage in the reach of C111 between S177 and S18C. The hydrogeological system at the study site consists
166 of the Biscayne aquifer which is a highly permeable shallow unconfined aquifer with hydraulic
167 conductivities reported to exceed 10,000 m/day, which explains the high connectivity between the canals
168 and the aquifer (Chin, 1991). The shallow nature of the water table implies that evaporation from the
169 groundwater could impact soil water content. The topography at this site is essentially flat with elevation
170 ranging approximately between 1.2 to 2.0 m above sea level NGVD 29. The climate is subtropical with

171 dry season (November to May), which is the growing season for vegetables, and wet season (June to
172 October). Approximately two thirds of all the rain (average annual rainfall ranges between 1100 to 1524
173 mm) is received during the wet season months.

174 The soil at the study site is very shallow (10 to 20 cm) with underlying limestone bedrock. According
175 to Nobel et al. (1996), the soils east of C111 vary and could be classified as either Krome and Chekika
176 very gravely loam (loamy skeletal, carbonatic, hyperthermic, Lithic Undorthents), or Biscayne Marl
177 (loamy, carbonatic, hyperthermic) based on their physical characteristics. We performed particle size
178 analysis using a standard 2-mm sieve and determined that the soils contain on average of 45% fine
179 fractions and 55% gravel. Color analysis using the Munsell soil color charts (Munsell soil charts, 2000)
180 and the color guide in Noble et al. (1996) identified the study site soils to be broadly characterized as
181 Chekika soil series.

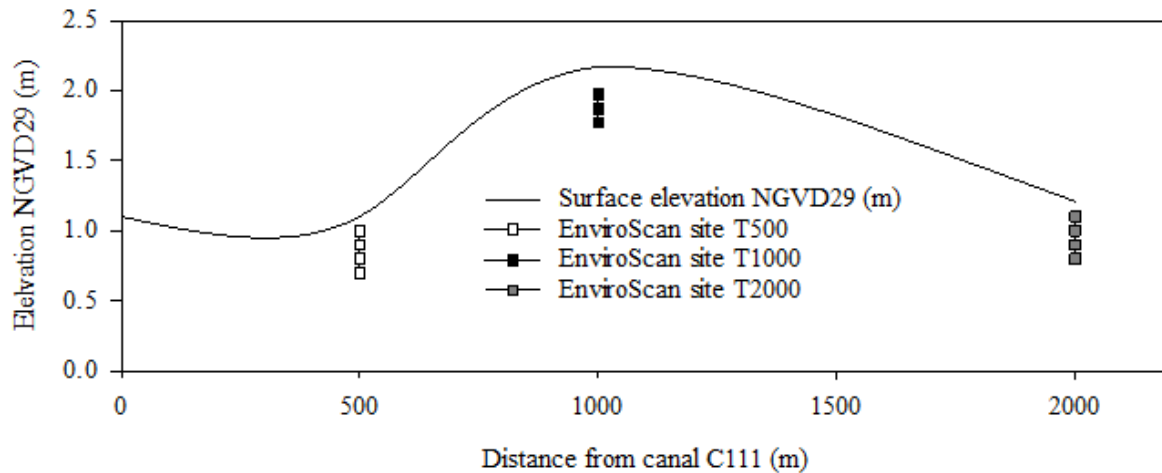
182 Three monitoring sites were used in this study located at 500, 1000 and 2000 m along a transect
183 perpendicular to canal C111, the three sites also had varying topographies and represented areas expected
184 to experience the greatest impact from the proposed raises in canal stage. Sites were selected to capture
185 differences in soil texture within our study area; this was done with a soil survey map and site visits. Sites
186 were also selected to ensure they were in privately owned agricultural low lying lands that were expected
187 to be impacted by the rises in water table elevation. For each site: i) GPS coordinates and elevation data
188 were collected, ii) groundwater wells were constructed and each was equipped with level loggers
189 (Levelogger, Gold Solinst Canada Ltd., 35 Todd Rd, Georgetown, Ontario, Canada) to record water table
190 elevation every 15 minutes, iii) multi-sensor capacitance probes (MSCP) (EnviroScan probes, Sentek
191 Technologies, Ltd., Stepney, Australia) were installed at each site to monitor soil and bedrock water
192 contents. Monitoring site locations are shown in Fig. 1; elevations are shown in Fig.2. Differences in the
193 length of times series at the three sites was due to differences in the dates of installation of the EnviroScan
194 probes (i.e., probes could only be installed when water was at least 50 cm below the ground surface) and

195 relocation of the probes due to initial poor installation. Site T500 was installed on August 25, 2010, while
196 sites T1000 and T500 were installed on January 21, 2011.



197

198 Figure 1. . Map of the study area showing Everglades National Park, Taylor Slough, Florida Bay,
199 SFWMD canal network and low lying agricultural areas east of canal C111 in south Florida



200

201 Figure 2. Showing a topographic changes along transect T and the elevation of the EnviroScan sensors at
 202 the three sites.

203 2.2 Soil and bedrock water contents monitoring

204 Two EnviroScan probes were installed at each site for a total of six. Each access tube with a diameter
 205 of 50.5 mm housed four sensors positioned at various elevations as shown in Fig. 2. The elevations
 206 correspond to 10, 20, 30 and 40 cm from the ground surface at each site. The top 20 cm typically
 207 represent the scarified soil layer which is used for crop production and the lower 20 cm represent the
 208 underlying limestone bedrock in which plant roots cannot penetrate. To minimize the problem of air
 209 pockets, we used fast setting cement slurry between the access tube and the soil. The purpose of installing
 210 two EnviroScan probes at the same location was to ensure that at least one probe was functioning at any
 211 given time. Due to the shallowness of the limestone bedrock at all the study sites, a motorized drill was
 212 required to bore a hole that held the access tube in a vertical position. Water content data were logged
 213 every 15 minutes and were downloaded weekly and averaged daily.

214 EnviroScans are an example of capacitance based sensors which measure frequency of an oscillating
 215 electrical circuit. The oscillator is coupled electrically to capacitive elements that are made of two metal
 216 cylindrical electrodes. The electrode system is arranged so the soil becomes part of the dielectric medium
 217 affected by the fringing electromagnetic field. Volumetric soil water content affects the electrical

218 permittivity of the soil which in turn affects the capacitance causing the oscillation frequency to shift
 219 (IAIA, 2008) since the soil dielectric constant is a combination of mineral particles (2-4), water (80), and
 220 air (1). According to Dean et al. (1987) the oscillatory frequency from the capacitance soil water sensor
 221 could be expressed eq. (1):

$$222 \quad F = \frac{1}{2\pi\sqrt{L}} \left(\frac{1}{C} + \frac{1}{C_b} + \frac{1}{C_c} \right)^{1/2} \quad (1)$$

223 Where C_b is the total base capacitance and C_c is the total collector capacitance and these represent
 224 capacitances of internal circuit elements to which the electrodes are connected, L is the inductance of the
 225 coil in the circuit, and C is the capacitance of the soil access tube system. Therefore capacitance of the
 226 soil access tube system, C , can be expressed as a function of the soil dielectric constant (ϵ) and a value g
 227 representing the geometry of the sensor as shown in eq.(2).

$$228 \quad C = g \epsilon \quad (2)$$

229 Differences in oscillatory frequency among sensors at the same soil and bedrock water contents were
 230 eliminated by normalizing the oscillatory frequency values using values of frequency when the sensor
 231 was surrounded by water and air. The normalized oscillatory frequency is known as the scaled frequency
 232 (SF) and is estimated as in eq. 3. The manufacture default calibration equation (eq. 4) can be used to
 233 convert scaled frequency to volumetric soil water content (θ)

$$234 \quad SF = F - F_a / F_w - F_a \quad (3)$$

$$235 \quad \theta = (0.792 * SF - 0.0226)^{2.475} \quad (4)$$

236 where F is the oscillatory frequency value measured by the EnviroScan sensor, F_a is frequency value
 237 when the EnviroScan probe is surrounded by air, and F_w is the frequency value when the EnviroScan
 238 probe is surrounded by water. To avoid location specific calibration for each sensor, we use SF as

239 surrogate for θ for investigating the effect of various factors on soil and bedrock water contents and thus
240 did not use eq. (4). This approach was successfully applied by Ritter et al. (2009) when studying the
241 effect of various factors on hydrologic fluxes in a forest top soil using refractive index from time-domain
242 reflectometry (TDR) as a surrogate for volumetric soil water content. Gabriel et al. (2010) observed that
243 the manufacturer's calibration equation overestimated volumetric soil water compared to the locally
244 developed calibration equation. However, they noted that despite the overestimation of volumetric soil
245 water content, the manufacturer's equation was able to reproduce temporal soil water dynamics.
246 Therefore, if the goal is to measure relative changes in water content the manufacturer's default
247 calibration equation is sufficient.

248 **2.3 Measurement and estimation of hydrologic variables**

249 Hydrologic variables including canal stage, water table elevation NGVD29 m, rainfall (P), potential
250 evapotranspiration (ET_o) and groundwater evaporation (E) were measured or estimated to assess their
251 influence on soil and bedrock water content time series.

252 **2.3.1 Canal stage**

253 Canal stage data were measured at the S177 spillway for headwater (S177H) and tail water (S177T)
254 every 15 minutes but daily averages were used. Canal stage data were measured by the SFWMD and are
255 publically available from the online environmental database (DBhydro;
256 http://www.sfwmd.gov/dbhydroplsql/show_dbkey_info.main_menu). During the first phase of the C111
257 spreader canal project, the main operational adjustments will involve incrementally raising canal stage at
258 S18C (Fig. 1) which will result in increased stage in the reach of C111 between the spillways at S177 and
259 S18C.

260 **2.3.2 Water table elevation**

261 Water table elevation data were collected from three observation wells constructed at the three
262 monitoring sites. Water table elevation was measured by the University of Florida (UF) every 15 minutes
263 and averaged daily using a multi parameter pressure transducer at T1000 (Levelogger, Gold Solinst
264 Canada Ltd., 35 Todd Rd, Georgetown, Ontario, Canada). Atmospheric corrections were included using a
265 STS Barologger (Solinst Canada Ltd) in the well at T1000 (Fig. 1). Data were downloaded from the well
266 weekly and as a quality control procedure, water table elevations were also measured manually with a
267 Model 102 Laser water level well meter (Solinst, Canada Ltd). Wells T2000 (C111AE) and T500
268 (C111AW) were installed and operated by the SFWMD and published on DBHydro.

269 **2.3.3 Rainfall**

270 Gauge adjusted Next Generation Radar (NEXRAD) rainfall data used in this study were obtained
271 from the SFWMD. The United States National Weather Service operates two NEXRAD sites close to the
272 study site (i.e., KBYX in Key West, FL and KAMX in Miami, FL) that provide 2 km x 2 km NEXRAD
273 rainfall data. There are tradeoffs between rainfall estimated by rain gauges and NEXRAD. Rain gauges
274 (e.g., tipping buckets) provide accurate point estimates of rainfall which are acceptable for frontal related
275 rainfall events. However, in South Florida where most of the rainfall is received in summer and summer
276 rainfall is dominated by conventional or tropical rainfall forming processes, rain gauges may fail to
277 accurately represent the orientation of the rainfall front or fail to capture the entire rainfall event (Pathak,
278 2008). On the other hand, measurement of rainfall by NEXRAD relies on the raindrop reflectivity which
279 could be affected by factors such as raindrop size and microwave signal reflection by other particles in the
280 atmosphere. Skinner et al. (2008) showed that the best of the two measurement methods is realized by
281 using rain gauge or tipping bucket data to adjust NEXRAD values.

282 **2.3.4 Ground surface potential evapotranspiration**

283 Ground surface reference evapotranspiration (ET_0) was computed from micrometeorological data
284 (i.e., solar radiation, temperature, relative humidity and wind speed) obtained from a Florida Automated

285 Weather Network (FAWN; <http://fawn.ifas.ufl.edu/>) station located approximately 10 km northeast of the
 286 study site at the Tropical Research and Education Center, Homestead, FL. The American Society of Civil
 287 Engineers (ASCE) standardized Penman–Monteith equation was used to estimate ET_0 values (ASCE,
 288 2005). We assumed a crop with the following characteristics transpiring at a potential rate: crop height
 289 (0.12 m), albedo (0.23), active leaf area index (1.44), and well illuminated leaf stomatal resistance (100.8
 290 s/m). We applied the tool REF-ET (Allen, 2011) to calculate the ASCE standardized ET_0 from weather
 291 data.

292 2.3.5 Evaporation from the water table

293 Flux due to water table evaporation may influence soil and bedrock water contents. Previous studies
 294 have shown that when canal influences are negligible, direct evaporation from the water table
 295 significantly contributes to water table declines in the Biscayne aquifer (Merrit, 1996; Chin, 2008). Two
 296 types of models are available to estimate evaporation from a water table: physically based models and
 297 empirically based models. In this study, the latter was used because the former requires detailed data such
 298 as coefficient of diffusion of water vapor through the soil and vapor pressure above the soil surface which
 299 were not collected. Empirical models simply relate water table evaporation rate to the depth of the water
 300 table below the ground surface and are used in groundwater studies (e.g., MODFLOW uses this approach;
 301 Chin, 2008). We used a model similar to that proposed by McDonald and Harbaugh (1988) (eq. (5)). Chin
 302 (2008) modified eq. (5) and obtained eq. (6) for south Florida conditions.

$$303 \quad \frac{E}{E_0} = \left(1 - \frac{d}{d_{cr}}\right), \quad d_{cr} = 100 * (170 + 8T), \quad d < d_{cr} \quad (5)$$

$$304 \quad \frac{E}{E_0} = \begin{cases} 1 & d \leq d_0 \\ 1 - \frac{d - d_0}{d_{cr}} & d_0 < d < d_{cr} \\ 0 & d \geq d_{cr} \end{cases} \quad (6)$$

305 where E is water table evaporation [mm/day], E_0 (same as ET_0) is the potential evaporation rate at the
 306 ground surface [mm/day], d is the depth of the water table below the ground surface [m], d_{cr} is the critical
 307 depth below which evaporation ceases [m], T is annual average air temperature [$^{\circ}\text{C}$] which is
 308 approximately 25°C in south Florida, d_0 is water table depth above which water table evaporation
 309 proceeds at potential rate i.e., at the rate similar to the ground surface evapotranspiration [m]. Chin (2008)
 310 proposed parameters d_0 and d_{cr} in eq. (6) at each observation well can be estimated from the least squares
 311 best fit of eq. (7) and the parameters described as eq. (8) and (9).

$$312 \quad \frac{E}{E_0} = \alpha - \beta d \quad (7)$$

$$313 \quad d_0 = \frac{\alpha - 1}{\beta} \quad (8)$$

$$314 \quad d_{cr} = \frac{\alpha}{\beta} \quad (9)$$

315 **2.4 Dynamic factor analysis**

316 DFA uses eq. (10) to describes a set of N observed time series (Lütkepohl, 1991; Zuur et al., 2003;
 317 Ritter and Muñoz-Carpena, 2006). The goal in DFA is to keep M as small as possible while still obtaining
 318 a good model fit. Including relevant explanatory variables helps to reduce some of the unexplained
 319 variability in the observed time series.

$$320 \quad s_n(t) = \sum_{m=1}^M \gamma_{m,n} \alpha_m(t) + \mu_n + \sum_{k=1}^K \beta_{k,n} v_k(t) + \varepsilon_n(t) \quad (10)$$

$$321 \quad \alpha_m = \alpha_m(t-1) + \eta_m(t) \quad (11)$$

322 where $s_n(t)$ is a vector containing the set of N time series being modeled (response variables), $\alpha_m(t)$ is a
323 vector containing the common trends (same units as the response variables), $\gamma_{m,n}$ are factor loadings or
324 weighting coefficients that indicate the importance of each of the common trends to each response
325 variable (unitless), μ_n is a constant level parameter for shifting time series up or down, $\nu_k(t)$ is a vector
326 containing explanatory variables, and $\beta_{k,n}$ are weighting coefficients for the explanatory variables
327 (regression parameters) which indicate the relative importance of explanatory variables to each response
328 variable (inverse units to convert $\nu_k(t)$ into response variable units), and $\varepsilon_n(t)$ and $\eta_m(t)$ are
329 independent, Gaussian distributed noise with zero mean and unknown diagonal covariance matrix. The
330 elements in the covariance matrix represent information that cannot be explained by the common trends
331 or the explanatory variables. The unknown parameters $\gamma_{m,n}$ and μ_n were estimated using the Expectation
332 Maximization (EM) algorithm that is described in Dempster et al. (1977) and Shumway and Stoffer
333 (1982). The common trends in eq. (11) were modeled as a random walk (Harvey, 1989) and were
334 predicted using the Kalman filter and EM algorithms. The regression parameters in eq. (10) are estimated
335 using the same procedure as used in linear regression (Zuur et al., 2003). DFA was implemented using a
336 statistical package called Brodgar Version 2.5.6 (Highland Statistics Ltd., Newburgh, UK).

337 The results from the DFA were interpreted in terms of the canonical correlations ($\rho_{m,n}$), factor
338 loading ($\gamma_{m,n}$), regression parameters ($\beta_{k,n}$) and agreement between modeled and observed soil and
339 bedrock water contents (i.e., expressed as scaled frequency). The goodness-of-fit between modeled and
340 observed soil and bedrock water contents were quantified using the Nash-Sutcliffe coefficient of
341 efficiency (C_{eff} ; Nash and Sutcliffe, 1970), the Akaike's Information Criteria (AIC ; Akaike, 1974) and the
342 Bayesian information criterion (BIC). C_{eff} provides an estimate of how well a model predicts an observed
343 data set, while AIC and BIC are relative measures of the goodness-of-fit of a statistical model. A model
344 with the C_{eff} closest to 1 and lowest AIC and BIC is the preferred DFA model. Cross correlations between

345 the soil and bedrock water content time series and common trends were measured using $\rho_{m,n}$. In our study
 346 $\rho_{m,n}$ close to unity implied that the common trend was highly associated with water content time series.
 347 Typically canonical correlations are classified as follows: $|\rho_{m,n}| > 0.75$, 0.5-0.75, and 0.3-0.5 as high,
 348 moderate, and weak correlations, respectively. The influence of the explanatory variables on water
 349 content time series were quantified using the magnitude of the $\beta_{k,n}$ coefficients and their associated
 350 standard errors which were used with a *t-test* to assess whether the response variable and explanatory
 351 variables were significantly related.

352 DFA was implemented sequentially by varying the number of common trends M until a minimum
 353 AIC and BIC and C_{eff} closest to one were achieved (Zuur et al., 2003). After identifying the minimum M ,
 354 different combinations of explanatory variables were introduced into the analysis until a combination of
 355 common trends and explanatory variables that resulted in the most parsimonious model with best good-
 356 of-fit indicators was achieved. The procedure followed here is similar to that described by Ritter et al.
 357 (2009).

358 **2.4.1 Explanatory variables**

359 Soil and bedrock water content time series are autocorrelated (Kaplan and Muñoz-Carpena, 2011)
 360 while evapotranspiration and rainfall time series are not. For example, soil and bedrock water contents at
 361 time t will depend on antecedent soil and bedrock water contents at time $(t-1)$ whereas the rainfall today
 362 does not depend on rainfall yesterday. Therefore in order to relate the soil and bedrock water content time
 363 series and evapotranspiration and rainfall time series, we calculated a new variable called net cumulative
 364 recharge (R_{net}) using eq. 12.

$$365 \quad R_{net} = \sum_{t=1}^t P_t - \sum_{t=1}^t E_{o_t} \quad (12)$$

366 where P_t is the total rainfall for day t (mm) and E_{ot} is the potential evapotranspiration on day t (mm/day).
367 Cumulative water table evaporation was also used instead of daily values. To minimize multi-collinearity
368 of explanatory variables, we used mean water table elevation instead of water table elevation at each well.
369 Before proceeding with the DFA, multi-collinearity of explanatory variables was quantified by computing
370 variance inflation factors (VIFs) for each explanatory variable (Zuur et al., 2007).

371 **2.5 Simple predictive regression model for soil water content**

372 The simple regression model was developed from a DFA model having the minimum number of
373 common trends required to explain underlying common patterns in the eleven time series and explanatory
374 variables with significant influence on modeled soil water and bedrock water content time series. To
375 enable practical use of the simple model, DFA was performed again for the identified model using non-
376 normalized/non-standardized time series. After estimating the parameters through DFA the common
377 trends were ignored in the model to derive a simple expression relating identified significant explanatory
378 variables and soil and bedrock water contents. The period from August 25, 2010 to December 2011 was
379 used to develop the regression model while the data from December 01, 2011 to June 30, 2012 was used
380 to validate the new simple model. The developed simple model was then applied to predict the impact of
381 a 6, 9 and 12 cm increase in canal stage on soil and bedrock water contents at the study sites.

382 **3. Results and discussion**

383 **3.1 Visual exploratory analysis of experimental time series**

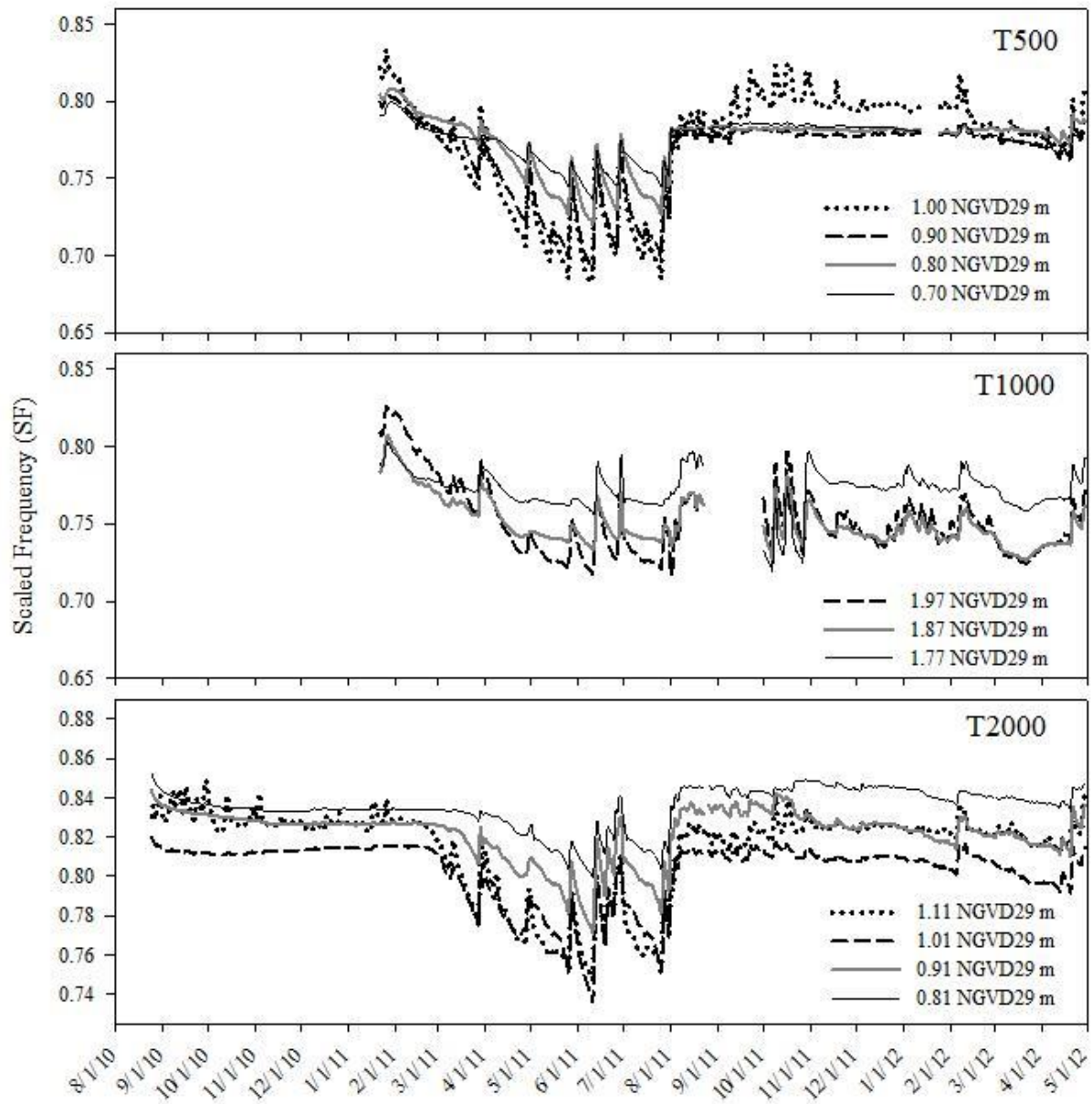
384 Visual inspection of soil and bedrock water content time series expressed as SF indicates that there
385 were some common patterns in the temporal variation of soil and bedrock water contents at the three sites
386 (T500, T1000 and T2000) along the transect perpendicular and east of canal C111. From February 2011
387 to July 2011, soil and bedrock water contents gradually decreased at all monitoring elevations and all sites
388 (Fig. 3). The gradual decrease in soil and bedrock water contents corresponded to the decline in canal
389 stage and water table elevation (Fig. 4). The period from April to August was characterized by

390 pronounced drying and wetting cycles at all sites. The wetting or spikes in soil and bedrock water
391 contents in this period correspond to the start of the rains while the drying cycles correspond to the
392 increasing potential evapotranspiration during the same period (Fig. 4). The period from late March to
393 July corresponds to the end of the growing season and beginning of the wet season. From August 2011 to
394 February 2012, soil and bedrock water increased corresponding to stage operation criteria within the canal
395 network that enhances water storage in the system.

396 However, there were observed differences in temporal soil and bedrock water variability at the three
397 monitoring sites along the transect. Site T500 which is the shallowest and closest to the canal exhibited
398 lack of temporal variation in bedrock water content at elevations less than 0.9 m NGVD29 while soil
399 water content at 1.0 m NGVD29 exhibited temporal variation in the same period probably due to
400 irrigation during the growing season. Site T1000 (i.e., approximately 1000 m from canal C111) exhibited
401 the least increase in water content between March 2011 and June 2012. Unlike sites T500 and T2000, the
402 trends in soil and bedrock water contents at T1000 were not identical to the temporal variation in canal
403 stage or water table elevation suggesting micro-topography within the field might be affecting soil and
404 bedrock water contents since this site had the highest elevation along the transect (Fig. 2). At site T2000
405 (i.e., approximately 2000 m from canal C111), soil and bedrock water contents for the periods between
406 August 2010 to March 2011 and August 2011 to February 2012 were similar characterized by small
407 temporal variation similar to those exhibited at site T500. Sites T500 and T2000 have very similar
408 elevation (1.1 and 1.2 m NGVD29 respectively) implying that topography or ground surface elevation
409 might exert a stronger influence on temporal variation of soil and bedrock water contents compared to
410 distance from the canal. Differences also existed at the different monitoring elevations with bedrock water
411 content generally higher at the lowest elevation at each site. Other reasons for observed differences in
412 water content at the different sites could be a combination of several factors such as differences in soil
413 surface conditions, soil and limestone bedrock heterogeneity (specifically differences in soil water

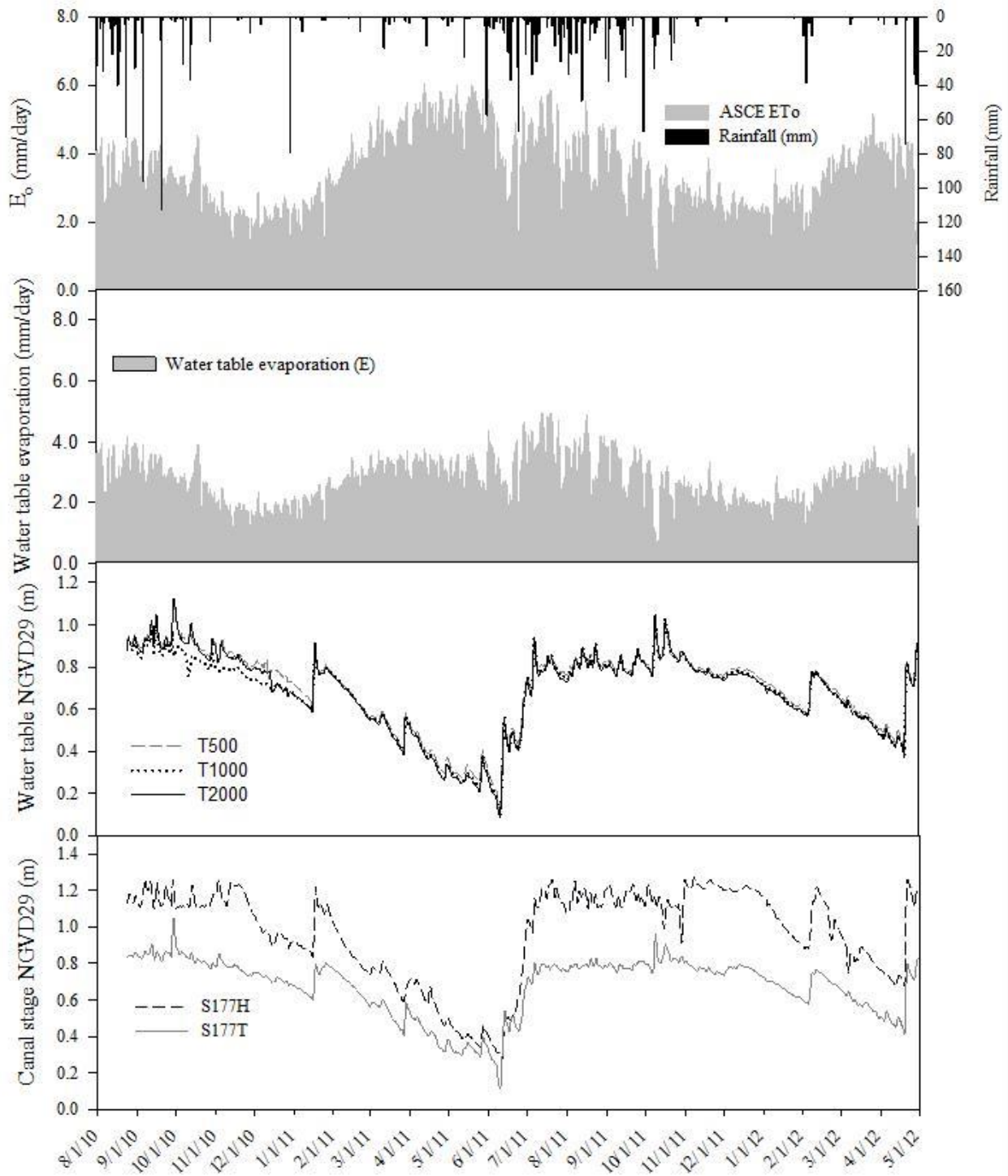
414 retention and unsaturated hydraulic conductivity) and differences in the environments surrounding the
415 EnviroScan access tubes.

416 All the hydrologic variables monitored (Fig. 4) exhibited seasonal variations with rainfall increasing
417 during wet season (May to October) resulting in increased water table elevation and canal stage. ET_o also
418 increased during the wet season. In turn, decreased depth to water table and increased ET_o resulted in
419 increased E (Fig. 4). The water table evaporation parameters for eq. (6) were computed following the
420 procedure described by Chin (2009) in which steady declines in water table elevation particularly in the
421 dry season when canal stage was maintained relatively constant are assumed to be caused by water table
422 evaporation. Using data from a total of six wells (i.e., the 3 wells along transect T and 3 additional wells
423 approximately 1 km north of the transect) within the vicinity of the study area, we obtained an average
424 critical depth of 1.94 m which is within the range of 1.5 to 2.9 earlier reported by Chin (2009). We
425 obtained a value of 0.59 m for the depth above which water table evaporation proceeds at the potential
426 rate which is approximately half the average value of 1.4 reported by Chin (2009). The water table
427 elevations at the three monitoring sites were very similar and also corresponded to the temporal variations
428 in canal stage on the tail water side of the spillway at S177.



429

430 Figure 3. Temporal variation in scaled frequency (i.e., soil and bedrock water contents) at three sites (i.e.,
 431 T500, T1000 and T2000 with soil and bedrock water contents monitored at different elevations using
 432 EnviroScan probes) along a transect perpendicular to C111 on the tail water side of the spillway at
 433 structure S177 during the period August 2010 to June 2012.



434

435 Figure 4. Temporal variation in hydrologic factors evaluated for their influence on soil and bedrock water
 436 contents at the study site during the period August 2010 to June 2012.

437 **3.2 Response and explanatory variables**

438 Visual inspection indicated that seasonality affects temporal variation of both response variables (i.e.,
439 soil and bedrock water contents at different elevations) and explanatory variables (i.e., ET_o , rainfall P ,
440 water table elevation, E and canal stage). We attempted to remove seasonality effects through seasonal
441 standardization following procedures described by Salas (1993), but this approach was abandoned since it
442 resulted in poor model fit compared to the models in which seasonal effects were assumed to be masked
443 in the common trends (i.e., average $C_{eff} < 0.7$ and $C_{eff} > 0.9$, respectively). The poor model fit could be
444 attributed to loss of information resulting from seasonal standardization. Ritter et al. (2009) also reported
445 improved DFA model fit after back transforming refractive index data from a TDR as a surrogate for soil
446 water content compared to seasonally standardized refractive index.

447 To facilitate interpretation of factor loadings and comparison of regression parameters as suggested
448 by Zuur et al. (2004), all the time series were normalized. Therefore, the DFA results presented in
449 reference to objective 1 are based on normalized time series data. Prior to performing the DFA,
450 multicollinearity in explanatory variables was quantified by calculating Variance Inflation Factor (VIFs)
451 for each explanatory variable. Threshold VIF of 5 was set as the highest, high values of VIF indicate
452 multicollinearity in the explanatory variables which makes interpretation of regression results difficult
453 (Ritter et al., 2009). As expected there was high multi-collinearity between water table elevation time
454 series for different wells (VIFs > 30), but this was considerably reduced when mean water table elevation
455 at the three sites was used instead (i.e., VIFs < 2). There was also high multi-collinearity between
456 headwater and tail water canal stages at S177 (VIFs > 8) implying that these two time series could not be
457 used as explanatory variables in the same DFA model. Mean water table elevation was also correlated to
458 canal stage S177 (VIFs > 10) probably due to the high hydraulic connectivity between C111 and Biscayne
459 aquifer. The correlation coefficient between canal stage and water table elevation time series was greater
460 than 0.9.

461 **3.3 Common trends**

462 We developed the DFA model by exploring common trends and explanatory variables in relation to
463 the 11 observed water content time series. Results of the DFA model selection are summarized in Table 1.
464 We used the *AIC*, the *BIC* (which penalizes more strongly for over parameterization than the *AIC*) and the
465 C_{eff} statistic for deciding which of the DFA models with zero explanatory variables best described the
466 response time series. Ten was the maximum number of common trends used to describe common
467 variability in the 11 response water content time series. However, the goal of DFA is to minimize the
468 number of common trends while maintaining a good model fit. Several models consisting of fewer
469 numbers of common trends and noise were tested and model 4 with five common trends was determined
470 to be the model with the minimum number of common trends required to describe the 11 response time
471 series. Model 4 was selected since using $M > 5$ resulted in negligible improvement in model goodness-of-
472 fit measures while increasing the number of parameters to be interpreted. The three common trends with
473 high ($|\rho_{m,n}| > 0.75$) to moderate ($0.5 < \rho_{m,n} < 0.75$) canonical correlations particularly at sites T500 and
474 T2000 are shown in Fig. 5. Common trends 2 and 3 exhibited minor cross correlation with water content
475 time series as measured by $\rho_{m,n} < 0.5$ at all the sites and in the interest of brevity are not presented.

476 Visually, the unexplained variation in soil and bedrock water contents described by the common
477 trends in Fig. 5 is similar to the seasonal variation of soil and bedrock water contents at sites T500, T1000
478 and T2000 for the period August 2010 to August 2011. There was greater uncertainty as shown by a large
479 (95%) confidence interval from August 25, 2010 to January 21, 2011 which is due to missing data for
480 sites T500 and T1000 during this period. The first common trend exhibited high positive ($|\rho_{1,n}| \geq 0.75$)
481 correlation with soil and bedrock water content time series at sites T500 and T2000 with low surface
482 elevation (1.1 and 1.2 m NGVD29, respectively) compared to the moderate to weak correlation at site
483 T1000 with ground surface elevation of 2.17 m NGVD29. Indicating that in addition to other factors, such

484 as irrigation during the growing season, micro-topography within the field influences temporal variations
 485 in soil water content as it governs the effect exerted by the water table.

486 Table 1. Dynamic Factor Analysis (DFA) models tested based on the following goodness-of-fit measures:
 487 AIC, BIC and C_{eff}

Model	No. of common trends	Explanatory variables	No. of parameters	AIC ¹	BIC ²	C_{eff} ³
Step I (DFA model with K=0)						
1	2	None	98	-2690.50	-2041.75	0.68
2	3	None	107	-4654.23	-3945.90	0.84
3	4	None	115	-5830.21	-5068.92	0.88
4	5	None	122	-6901.47	-6093.84	0.97
5	6	None	128	-7028.76	-6181.40	0.97
6	8	None	137	-7263.94	-6357.01	0.97
Step II (DFA model with K>0)						
7	5	R_{net} ⁴ ,	133	-7018.644	-6138.193	0.97
8	5	R_{net} , E ⁵	144	-7797.525	-6844.255	0.98
9	5	S177T ⁶	133	-7340.981	-6460.530	0.97
10	5	S177T, R_{net}	144	-7542.680	-6589.410	0.97
11	5	R_{net} , E , MWT ⁷	155	-8052.436	-7026.346	0.98
12	5	MWT, R_{net}	144	-7444.030	-6490.761	0.97
13	5	R_{net}, E, S177T	155	-7922.346	-6896.257	0.98

488 ¹AIC Akaike information criterion

489 ²BIC Bayesian Information Criterion

490 ³ C_{eff} Nash-Sutcliffe coefficient calculated based all the nine observed time series

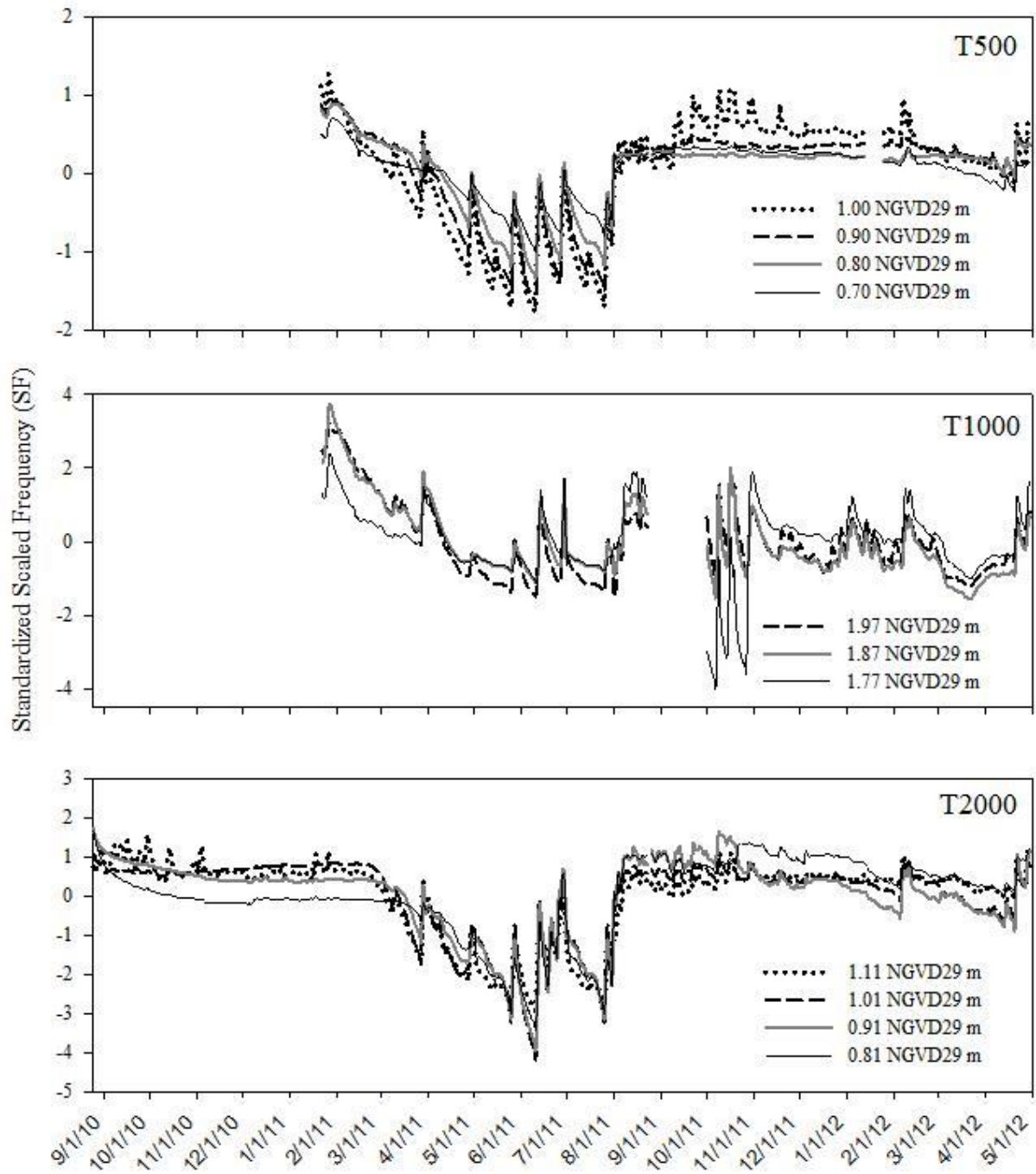
491 ⁴Cumulative net surface recharge

492 ⁵ R_{net} Cumulative water at table evaporation

493 ⁶S177T Canal stage in C111

494 ⁷MWT Mean water table evaporation

495



496

497 Figure 5. Common trends with 95% confidence interval describing unexplained temporal variation in
498 scaled frequency as a surrogate for soil and bedrock water content and the canonical correlation for
499 quantifying the correlation between water time series and the common trends, in the nomenclature for site

500 names the number represents distance from the canal in m, and the numbers in the parenthesis represent
501 elevation NGVD 29 m.

502 **3.4 Relative contribution of explanatory variables**

503 Introducing net surface recharge, water table evaporation, and mean water table elevation or C111
504 canal stage to model 4 resulted in the best models (11 and 13). Inclusion of explanatory variables in the
505 DFA model also produced regression parameters ($\beta_{k,n}$) and since response and explanatory variables
506 were normalized, the regression parameters were used to quantify the relative influence of each
507 explanatory variable on the modeled soil and bedrock water content time series. It is worth noting that
508 substituting mean water table elevation in model 11 with canal stage as in model 13 resulted in *AIC* and
509 *BIC* that were not substantially different and similar goodness-of-fit indicator (Table 1). Since part of the
510 motivation for this research was to assess the effect of canal stage management on soil and bedrock water
511 contents, further analysis was made on model 13 because canal stage data have a more consistent record
512 compared to water table elevation data. At the study site, canal stage can be used as a good approximation
513 to water table elevation due to the high permeability of the aquifer.

514 Model 13 fitted plots are shown in Figs. 6 to 8; these figures indicate that DFA modeling was
515 successfully applied to describe temporal variations in soil and bedrock water contents at all three
516 monitoring sites and elevations ($C_{eff} > 0.9$). Results in Table 2 indicate that net surface recharge (R_{net}) had
517 a significant influence (t value > 2) on the temporal variation of soil and bedrock water contents at sites
518 T500, T1000, and T2000 but was not significant at lower elevations at sites T1000 and T2000 as shown (t
519 value < 2). The significance of R_{net} could be attributed to rainfall (P) patterns in the study area in which
520 two thirds of the P was received in the wet season (SFWMD, 2011) and these large amounts of net water
521 input to the vadose zone are sufficient to maintain soil and limestone bedrock near saturation, while
522 absence of P in the dry season was responsible for the dry conditions. Lack of significance at lower

523 elevations at sites T1000 and T2000 could be attributed to heterogeneity in soils and bedrock (e.g.,
524 differences in hydraulic conductivity), and differences in surface cover which influence ET_o .

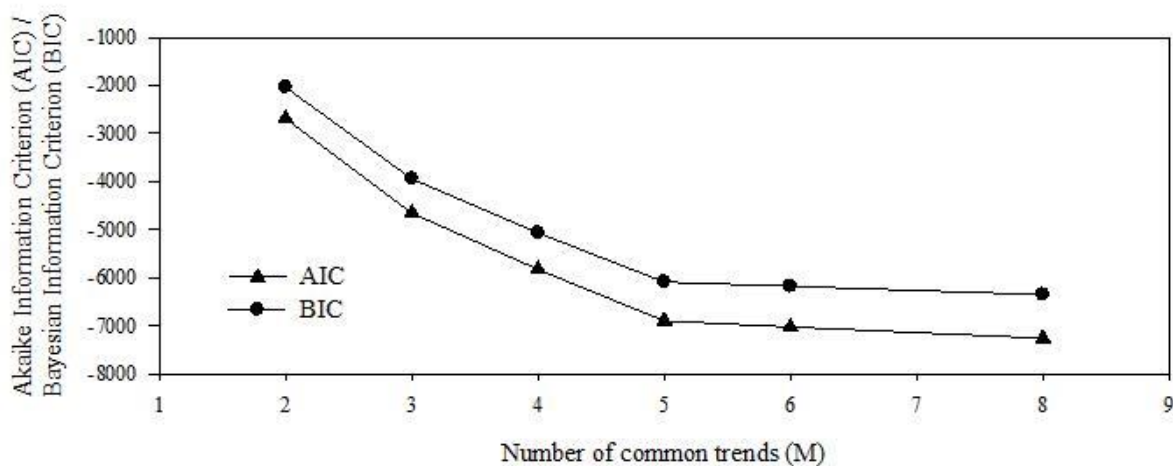
525 Water table evaporation was found to not significantly influence temporal variation of soil and
526 bedrock water contents (t value <2) at all the sites monitored. The non-significant effect of water table
527 evaporation on soil and bedrock water content could be attributed to the fact that there is sufficient water
528 for evaporation due to the shallow water table. However, the negative effect was stronger at site T1000,
529 the negative effect is due to the fact that water table evaporation is a net loss from the vadose zone
530 system. The small positive water table evaporation regression coefficient at T1000 and T2000 (Table 2)
531 could be attributed to computational numerical errors. These results are worth highlighting given the fact
532 that meteorological based methods for estimating ET_o like Penman Monteith equation are criticized for
533 ignoring evaporation from the shallow water table meaning they might under estimate total ET_o losses.
534 These observations could be attributed to that fact ET_o in such cases is not limited by water availability
535 but by available energy only.

536 C111 canal stage on the tail water side at the S177 spillway (Fig. 1) had the strongest influence on
537 soil and bedrock water content temporal variations (t value >7) for most sites. This finding is significant
538 because it confirms the hypotheses that the shallow water table and canal stage are highly connected and
539 that canal stage can be used to predict soil water content at a given location. From a hydrologic
540 perspective, these results were expected because in this case canal stage is used an approximation for the
541 shallow water table which serves as the lower boundary condition for the vadose zone and therefore
542 regulates available storage during the rainy season. Based on the relative magnitudes of the regression
543 coefficients (Table 2), the overall contribution of canal stage on the respective soil and bedrock water
544 content time series is higher than that of net recharge.

545 The factor loadings ($\gamma_{1,n}$) for the five common trends are shown in Table 2, these represent the
546 influence of each common trend on the modeled soil and bedrock water content time series at the

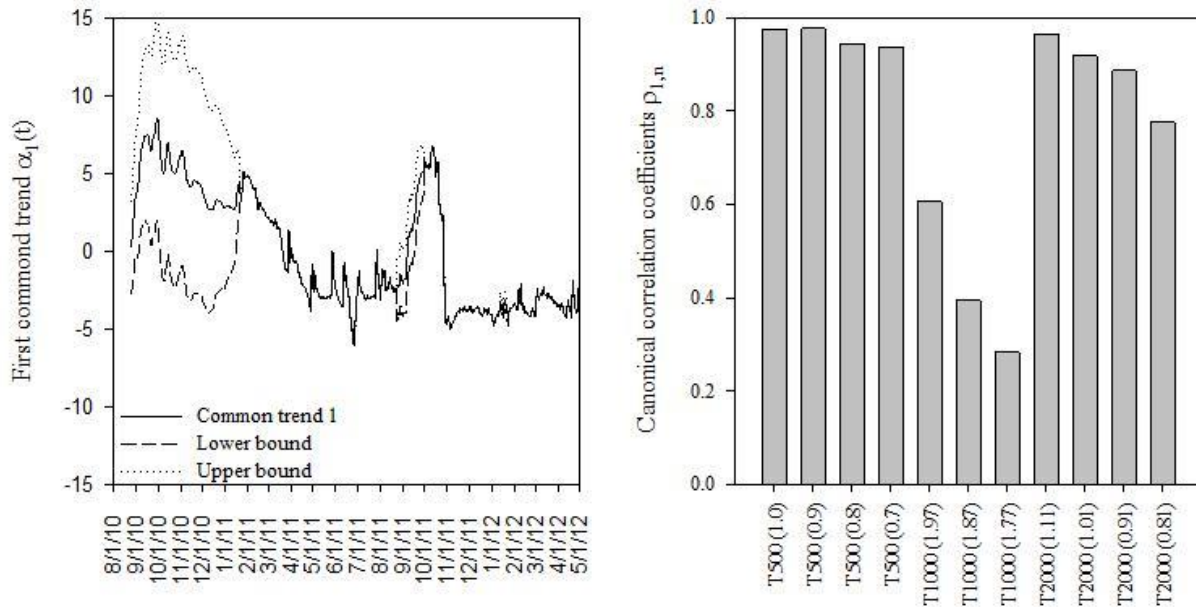
547 different monitoring sites and elevations. Since the time series in the DFA were normalized, the
 548 coefficients $\beta_{k,n}$ and $\gamma_{1,n}$ can be compared (Zuur and Pierce, 2004). The results indicate that trend 1 was
 549 very critical for describing unexplained variation in soil water dynamics at site T2000, while common
 550 trends 2 and to a lesser extent 3 were more critical for describing unexplained variation in soil water
 551 content at site T1000. Site T500 was sufficiently described by the explanatory variables and constant level
 552 parameters given their magnitudes were larger compared to the $\gamma_{1,n}$. Trends 4 and 5 had minor effects at
 553 all the monitoring sites.

554 Overall at all the sites, compared to regression coefficients and the constant level parameters,
 555 common trends had less influence on soil and bedrock water dynamics. However, since the values of the
 556 factor loadings are not zero (i.e., they account for some unexplained variability) especially at T2000 and
 557 site T1000, this implies that the information provided by the hydrologic variables used as the explanatory
 558 variables in the DFA models only account for part of the unexplained variability in the temporal variation
 559 of the soil and bedrock water contents. Other information such as irrigation, differences in soil surface
 560 conditions, differences in the environment surrounding the EnviroScan access tube, and variation in soil
 561 hydraulic properties not considered in this study might account for part of the remaining unexplained
 562 variability.



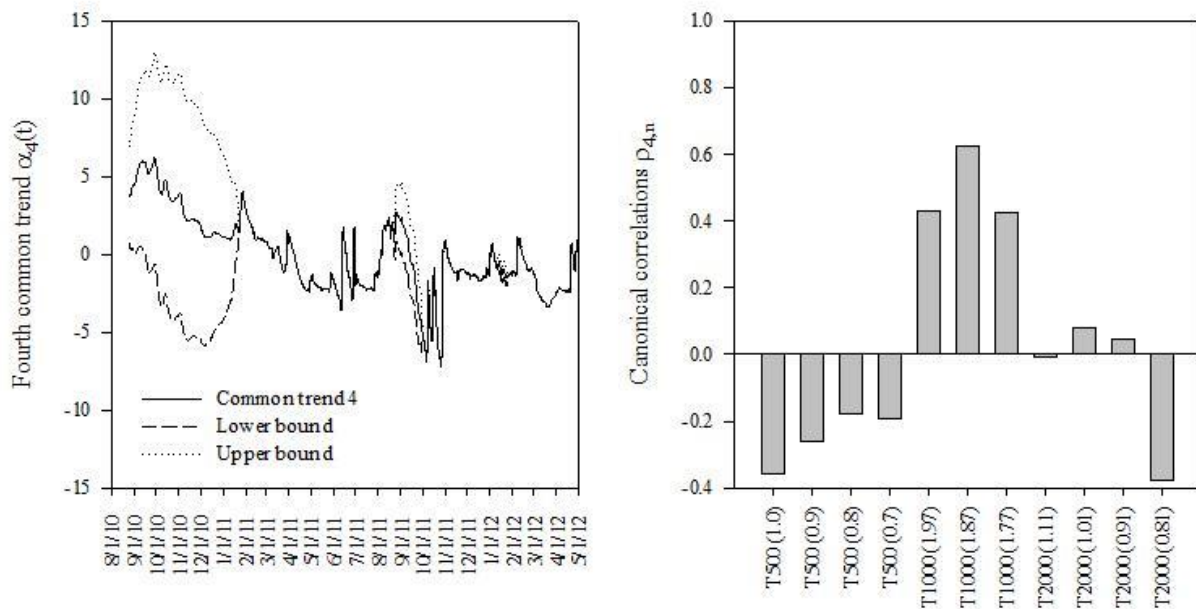
563

564 Figure 6. Fitted Dynamic Factor Model (DFM) and observed temporal variation in scaled frequency (used
 565 as a surrogate for soil and rock water) in gravely loam soils and limestone bedrock at a site located 500 m
 566 along a transect from C111 and the numbers in the parentheses indicate elevations.



567

568 Figure 7. Fitted Dynamic Factor Model (DFM) and observed temporal variation in scaled frequency
 569 (used as a surrogate for soil and rock water) in gravely loam soils and limestone bedrock at a site located
 570 1000 m along a transect from C111 and the numbers in the parentheses indicate elevations.



571

572 Figure 8. Fitted Dynamic Factor Model (DFM) and observed temporal variation in scaled frequency
 573 (used as a surrogate for soil and rock water) in gravely loam soils and limestone bedrock at a site located
 574 2000 m along a transect from C111 and the numbers in the parentheses indicate elevations.

575 Table 2. Dynamic Factor Analysis results for model 13 with 5 common trends and 3 explanatory
 576 variables

s_n	$\gamma_{1,n}$	$\gamma_{2,n}$	$\gamma_{3,n}$	$\gamma_{4,n}$	$\gamma_{5,n}$	μ_n	β_{Rnet}	β_E	$\beta_{C111stage}$	C_{eff}
¹ T500 (1.0)	0.05	0.02	0.04	-0.02	-0.03	0.28 (0.6)	0.34 (6.9)	0.00 (0.0)	0.24 (8.8)	0.93
T500 (0.9)	0.05	0.06	0.03	-0.04	-0.05	0.37 (0.5)	0.24 (3.5)	-0.14 (-0.3)	0.29 (8.3)	0.94
T500 (0.8)	0.04	0.06	0.03	-0.03	-0.04	0.34 (0.6)	0.20 (3.2)	-0.17 (-0.5)	0.22 (7.5)	0.90
T500 (0.7)	0.03	0.02	0.01	0.00	-0.01	0.13 (0.6)	0.18 (7.1)	-0.09 (-0.7)	0.13 (9.1)	0.90
T1000 (1.97)	0.04	0.16	0.13	-0.02	0.00	0.95 (0.9)	0.47 (3.1)	-0.53 (-0.7)	0.62 (8.7)	0.85
T1000 (1.87)	0.04	0.20	0.11	0.01	0.01	0.82 (0.8)	0.38 (2.1)	-0.61 (-0.8)	0.70 (8.5)	0.81
T1000 (1.77)	0.01	0.50	0.01	0.00	0.00	0.00 (0.0)	0.44 (1.1)	0.23 (0.1)	0.77 (4.6)	0.67
T2000 (1.11)	0.10	0.04	0.06	-0.07	0.01	0.07 (0.1)	0.13 (2.0)	0.05 (0.1)	0.50 (11.6)	0.99
T2000	0.13	0.05	0.06	-0.02	0.06	-0.09 (-0.1)	0.03 (0.3)	-0.03 (0.0)	0.68 (13.2)	0.90

(1.01)											
T2000											
(0.91)	0.17	0.03	0.06	0.01	-0.01	-0.12 (-0.1)	0.05 (0.4)	-0.22 (-0.3)	0.71 (12.4)	0.93	
T2000											
(0.81)	0.16	0.04	-0.03	-0.02	-0.02	-0.31 (-0.3)	0.08 (0.8)	0.02 (0.0)	0.46 (8.8)	0.96	

577 γ Factor loading corresponding to common trend 1 to 5 and observation, $n= 1, 2, 3, \dots, 11$

578 μ Constant level parameter in dynamic factor model with associated t -value in parenthesis

579 β Regression parameter corresponding to the 3 explanatory variables (net recharge [R_{net}], water table evaporation [E], and canal stage in C111 [C111stage]) with associated t -value in parenthesis

581 C_{eff} is Nash-Sutcliffe coefficient

582 ¹Site name nomenclature; T is refers to transect name T, number refers to distance from canal and number in parentheses refers to elevation NGVD29 m

584 n number of observations

585 3.5 Predicting soil and bedrock water contents using a simplified dynamic factor analysis based 586 model

587 To enable practical application of the DFA model, the common trends and two of the exploratory
588 variables included in model 13 were used in a new DFA model with non-standardized time series. This
589 new model was referred to as model 14. To further simplify model 14, we ignored the common trends to
590 derive a simple model that predicts soil and bedrock water contents as function of net recharge and canal
591 stage expressed as eq. 13

$$592 \quad SF(X, Z, t) = \beta_{R_{net}}(X, Z) R_{net}(t) + \beta_{C111}(X, Z) S177T(t) + \mu(X, Z) \quad (13)$$

593 where $SF(X, Z, t)$ is the SF at distance X from the canal, at elevation Z , and time t , other terms in
594 are previously described and varies with elevation and distance from the canal. The coefficients
595 for eq. 13 at all the sites and monitoring elevations are obtained from Table 3. The C_{eff} in Table 3 are
596 calculated based on eq. 13 with common trends removed. As expected, performance of the simple model
597 (eq. 13) was lower as shown by the reduction in C_{eff} (Table 3 and Figs. 9 to 10) compared to the DFA
598 models that include common trends particularly for site T1000.

599 Since factor loadings are not zero for all the trends (Table 3), this suggests that the explanatory
600 variables (net recharge and canal stage) used in the DFA model are not sufficient to explain all the
601 observed variations in the soil and bedrock water content time series. This is particularly true at site

602 T1000 which is affected by 4 out of the 5 common trends. Common trend number 2 appears to affect all
 603 the sites, it probably masks common variation such seasonal changes in rainfall, evapotranspiration and
 604 canal stage. Other common trends had minor effects at sites at all the other sites particularly at site T1000.
 605 The difference in response at site T1000 could be attributed to differences in elevation as shown in Fig. 2,
 606 site T1000 has a higher surface elevation and hence larger depth to water table.

607 The results in Table 3 also underscore the point that the effect of canal stage is stronger at low
 608 elevation sites T500 and T2000 compared to T1000. Thus, proper interpretation of modeling results in
 609 this area requires accurate quantification of micro-topography. Model performance ranged from good at
 610 sites T500 and T2000 to poor at site T1000 with root mean square error (RMSE) ranging from 0.005 to
 611 0.01. Figs. 9 to 10 show model performance during the calibration and validation periods, after removing
 612 the common trends, it can be seen that the simple model misses the peaks but is able to generally predict
 613 the temporal variation in soil and rock water content. The simple model (eq. 13) could be improved by
 614 using location specific water table elevation since canal stage is simply a good approximation of the mean
 615 water table elevation. Another simple sigmoidal regression model to predict soil and bedrock water
 616 contents from canal stage proposed by Kaplan et al. (2010a) was tried but later abandoned due to lower
 617 C_{eff} (i.e., averaging 0.2). This approach is based on the physical concept of drain to equilibrium. However,
 618 for our study site this condition was hard to achieve since during the dry season irrigation was taking
 619 place and in the rainy season there was frequent rainfall hence by removing data points corresponding to
 620 rainfall or irrigation, very few data points were left to develop a useful sigmoidal model for predicting soil
 621 and bedrock water content from canal stage.

622 Table 3. Dynamic Factor Analysis results for model 14 with 5 common trends and 2 explanatory
 623 variables implemented with non-standardized time series

S_n	$\gamma_{1,n}$	$\gamma_{2,n}$	$\gamma_{3,n}$	$\gamma_{4,n}$	$\gamma_{5,n}$	μ_n	β_{Rnet}	$\beta_{c11stage}$	C_{eff}	C_{eff}
¹ T500 (1.0)	-0.003	0.000	0.000	0.000	0.000	0.72	0.14	0.06	0.73	0.70
T500 (0.9)	-0.001	-0.004	0.000	0.000	0.000	0.72	0.11	0.04	0.61	0.62

T500 (0.8)	-0.001	-0.004	0.000	0.000	0.000	0.75	0.09	0.02	0.51	0.56
T500 (0.7)	-0.001	-0.002	0.002	0.000	0.000	0.76	0.07	0.01	0.81	0.74
T1000 (1.97)	0.003	-0.005	-0.002	0.000	0.001	0.73	0.10	0.02	0.61	0.15
T1000 (1.87)	0.002	-0.003	-0.001	0.000	0.001	0.74	0.05	0.01	0.51	0.13
T1000 (1.77)	0.001	-0.003	0.001	-0.002	0.000	0.77	0.02	0.00	0.25	0.11
T2000 (1.11)	0.000	-0.003	-0.002	0.000	0.000	0.76	0.08	0.06	0.70	0.61
T2000 (1.01)	0.000	-0.003	0.000	0.000	0.001	0.76	0.05	0.05	0.60	0.67
T2000 (0.91)	0.000	-0.002	0.000	0.000	0.001	0.77	0.03	0.04	0.67	0.63
T2000 (0.81)	-0.001	-0.001	0.000	0.000	0.001	0.80	0.02	0.02	0.65	0.61

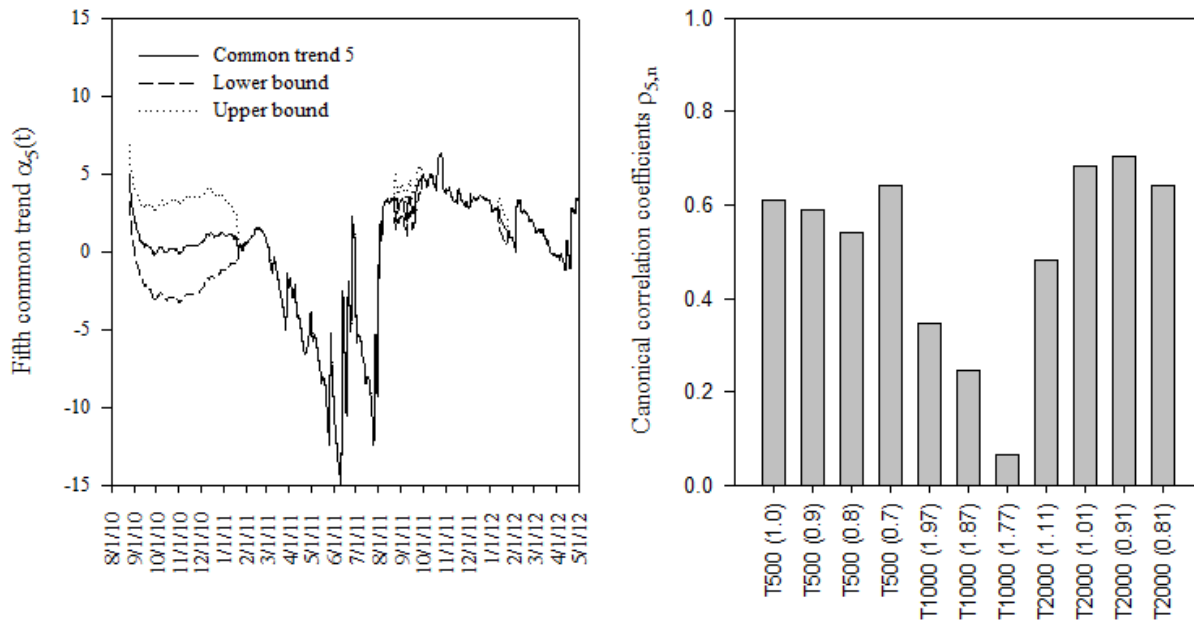
624 γ Factor loading in the dynamic factor model

625 μ Constant level parameter in dynamic factor model

626 β Regression parameter corresponding to the 2 explanatory variables (net recharge [R_{net}], and canal stage in C111 [C111stage])

628 ¹Nash-Sutcliffe coefficient are calculated after ignoring common trends

629 ²Nash-Sutcliffe coefficient during validation

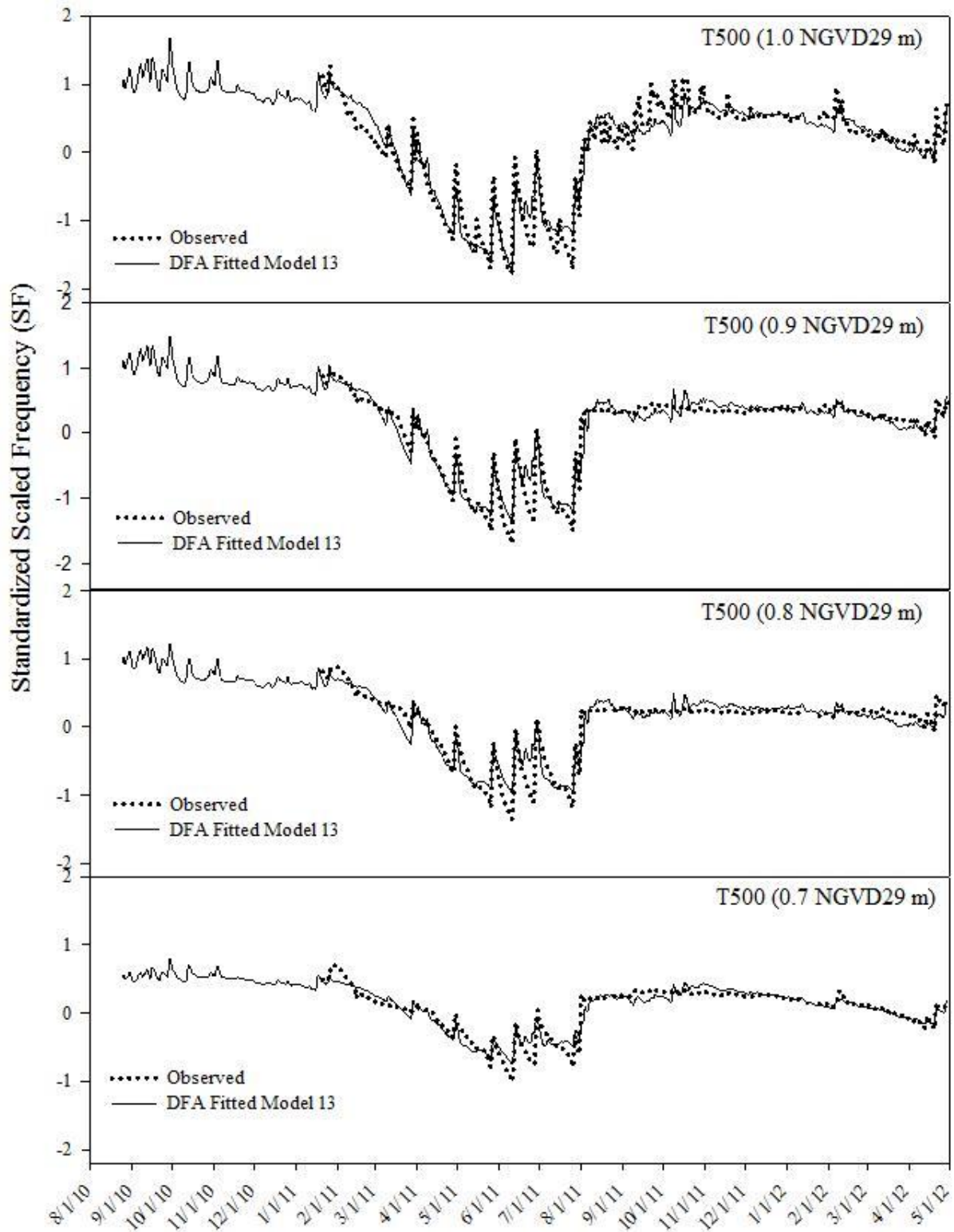


630

631 Figure 9. Performance of a simple model for predicting scaled frequency (used as a surrogate for soil and

632 bedrock water content) as a function of canal stage and net recharge at specific elevations in parentheses

633 NGVD29 at a site located 500 m along transect T from C111.



635 Figure 10. Performance of a simple model for predicting scaled frequency (used as a surrogate for soil
636 and bedrock water content) as a function of canal stage and net recharge at specific elevations in
637 parentheses NGVD29 at a site located 2000 m along transect T from C111.

638 **3.6 Assessing the impact of proposed operational changes in C111 canal stage management on soil** 639 **and bedrock water contents**

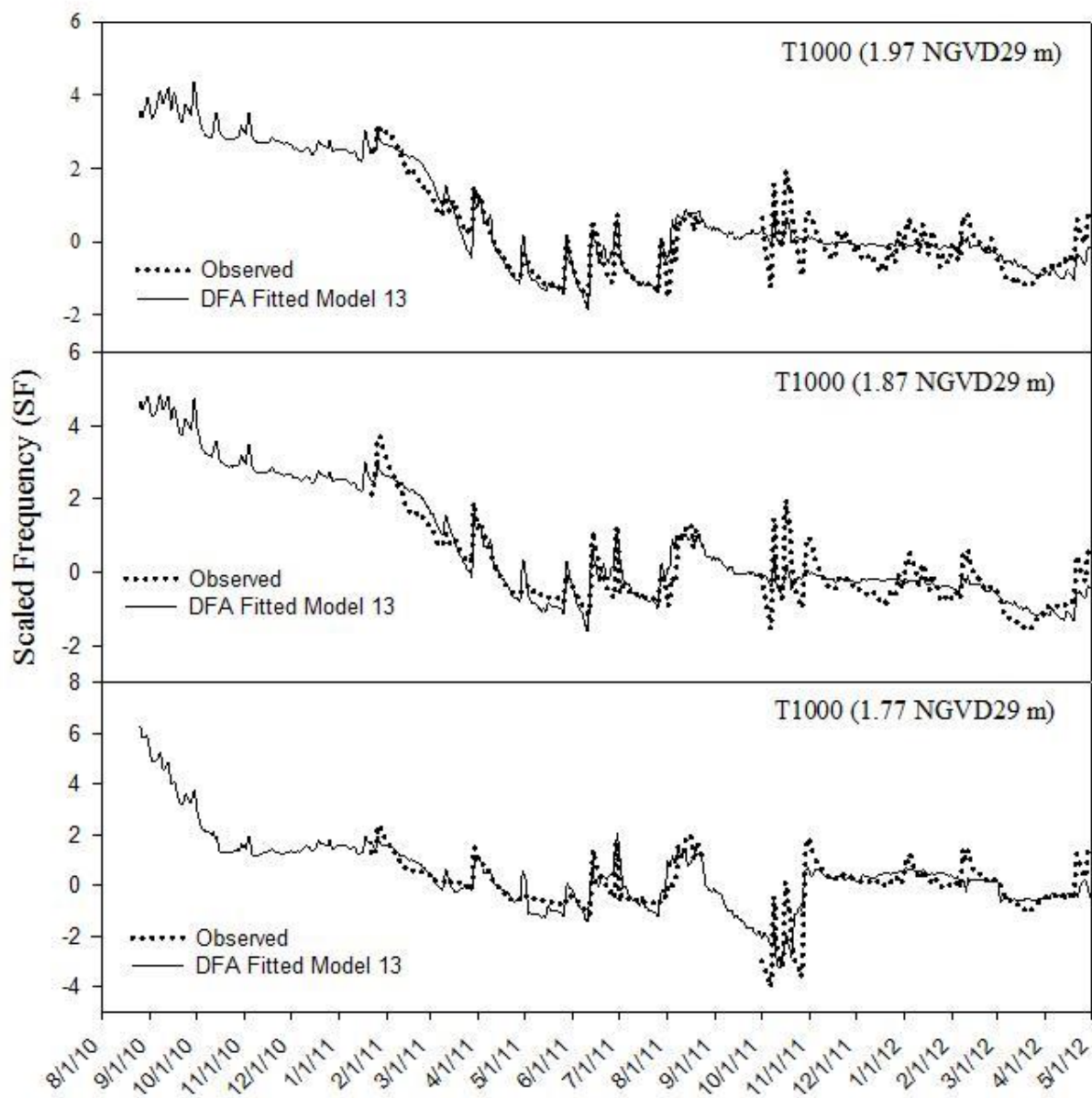
640 The low lying agricultural areas east of canal C111 are anticipated to experience the greatest
641 impact from the proposed changes in C111 stage operation (i.e., canal stage increases of 6, 9, and
642 12 cm); a simple DFA based regression model eq. 13 was proposed to predict the soil and
643 bedrock water contents as a function of canal stage. We considered the period from January 01,
644 2012, to June 30, 2012 for the analysis. Increases in canal stage were computed by simply adding
645 the proposed incremental rises in canal stage to the daily canal stage recorded at S177T while P
646 and ET_o from the original dataset were not changed.

647 The results from using this simplified DFA based model (Figs. 11 and 12) indicate that the
648 proposed increases in canal stage were predicted to have changes in daily mean SF for the study
649 period (i.e., which is used as a surrogate for soil and bedrock water contents) of <1% at all sites
650 and all elevations monitored. The range in daily SF differences was 0.065 to -0.024 and 0.075 to
651 -0.041 at sites T500 and T2000 respectively, which indicates that the simple model over
652 predicted and under predicted SF on certain days during the study period. However, note that the
653 daily differences in SF are not substantially large, this may be attributed to already high values of
654 soil and bedrock water contents observed in the area. On an event basis the potential to flood or
655 saturate the root zone would depend on the size of the storm and storm contingency planning for
656 lowering of canal stage in anticipation of heavy storms. Since we showed using DFA that soil
657 and bedrock water contents were significantly affected by canal stage and net recharge.

658 The simple model used in this evaluation was more accurate at sites T500 and T2000 and
659 therefore results at these two sites would be considered with less uncertainty. Soil and bedrock
660 water responses to incremental raises in canal stage were not computed for site T1000 since
661 results at this site would be considered less accurate (greater uncertainty) because model
662 performance was very poor at this site. Figs. 11 and 12 show that changes in soil and bedrock
663 water contents were more noticeable at the highest elevation. However, at the lowest elevations
664 monitored the difference between mean SF before and after all increments was zero at T500.
665 These observations could be attributed to the fact that low elevation sites are normally close to
666 saturation. For example, at site T500 (0.7) when water elevation was above the sensor (implying
667 saturated conditions), SF was recorded as 0.786 compared to average SF of 0.775 for the study
668 period meaning small changes in water table may not result in substantial changes in soil water
669 content since the pores are already near saturation.

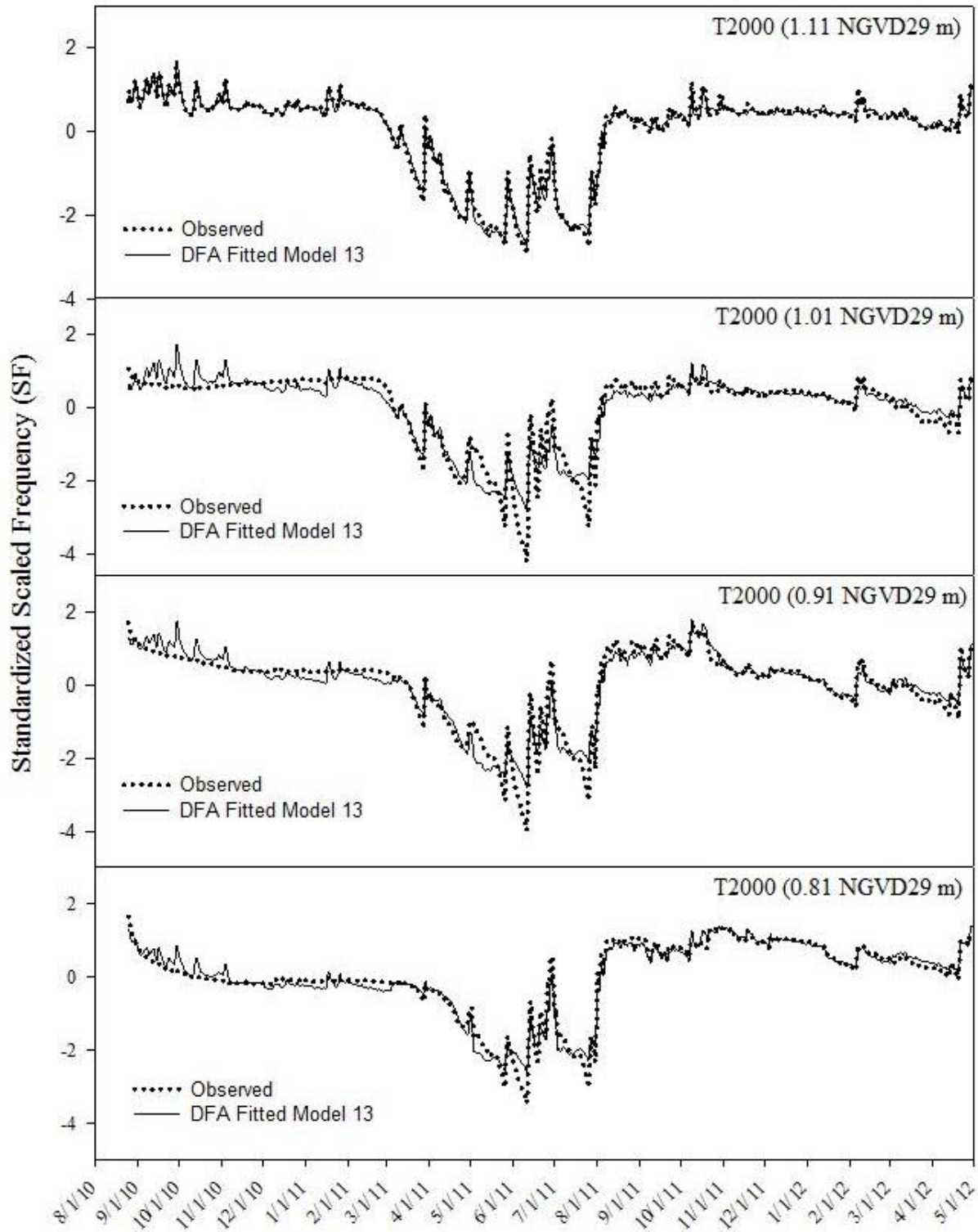
670 It is worth noting that the simple model developed above should be applied with the
671 following limitations in mind. The model does not account for water input from irrigation and
672 therefore would under predict soil and bedrock water content during the growing season, the
673 model also uses canal stage as an approximation for water table elevation at a specific location
674 although the two are usually close there may be deviations especially after large rainfall events, it
675 ignores water content drivers that were masked in the common trends, and lastly the simple
676 model ignores the effect of E which might vary based on micro-topography within the field as
677 well as differences in land surface cover conditions. Finally, although the simplified DFA based
678 model is empirical in nature, the results suggest it can be used as a preliminary tool to relate the
679 potential impacts of surface water management decisions on soil and bedrock water contents in
680 low lying farmlands adjacent to canal C111. This is because during the duration of the study, we

681 able to capture a wide range of variation in canal stage and water table elevation e.g., on June 10,
682 2011 we recorded canal stage and groundwater table elevation of 0.14 m NGV29 which is lower
683 than the optimum design stage of 0.6 m for the reach of C111 between S 18C and S177 under
684 current canal stage operational criteria. During the summer of 2011 (on October 09, 2011) we
685 recorded canal stage and groundwater levels as high as 0.9 and 1.02 m NGVD29 which is close
686 to the level supposed to trigger the spillway to open at S177 under current operational criteria.



687

688 Figure 11. Boxplots showing soil and rock water content as measured using scaled frequency at site T500
689 before and after 6, 9 and 12 cm increase canal at structure S18C along C111.



690

691 Figure 12. Boxplots showing soil and rock water content as measured using scaled frequency at site
692 T2000 before and after 6, 9 and 12 cm increase canal at structure S18C along C111.

693

694 **4.0 Summary and Conclusions**

695 The response of soil and bedrock water contents to incremental raises in canal stage proposed under
696 the C111 spreader canal project whose goal is to restore the hydrology of ENP while maintaining flood
697 protection in the adjacent agricultural areas was investigated using DFA. The study objectives were to use
698 DFA to identify the important factors driving temporal variation in soil and bedrock water content above
699 the shallow water table at the study site, develop a simple model for predicting soil water content as a
700 function of canal stage and assess the effect of the proposed incremental raises in canal stage on soil and
701 bedrock water contents. Five was the minimum number of common trends required to account for the
702 unexplained variation in the eleven observed soil and bedrock water content time series while producing
703 an acceptable model fit. Introduction of explanatory variables i.e., net recharge, water table evaporation,
704 and canal stage or water table elevation to the DFA model resulted in lowering AIC and BIC values while
705 C_{eff} values did not substantially change. Evaluation of the regression coefficients indicated that net
706 recharge and canal stage had significant effects on temporal variation of soil and bedrock water contents
707 while the effect of water table evaporation was non-significant. Based on the magnitude of the regression
708 coefficients, canal stage had the greatest influence on the temporal variation of soil and bedrock water
709 contents at all elevations and distances from the canal at the locations monitored. The effect of canal stage
710 and mean water table elevation in the DFA model was similar confirming the high hydraulic connectivity
711 between the canal and Biscayne aquifer.

712 Based on the high connectivity between surface water in the canal and Biscayne aquifer, a simple
713 DFA based regression model (DFA model in which the common trends were removed), was developed to
714 predict soil and bedrock water contents as a function of canal stage and net recharge at various elevations.
715 The performance of the simplified regression model was described as good to acceptable at sites with low
716 elevation (i.e., water table elevation within 1m from the ground surface) and poor at the location at with
717 water table depth greater than 1.5 m. These findings highlight the effect of micro-topography within the
718 field on soil water content. The study also revealed that factor loadings were not zero for all the common

719 trends suggesting that the explanatory variables (net recharge and canal stage) used in the DFA model are
720 not sufficient to explain all the observed variations in the soil and bedrock water content time series.

721 The effect of the proposed 3 incremental raises in canal stage on soil and bedrock water content was
722 simulated using the developed simple DFA based regression model for a total of 181 days beginning
723 January 01, 2012. The results based on the data collected indicate that the proposed raises in canal stage
724 would result in negligible changes in average soil and bedrock water contents at low elevations monitored
725 in this study based. Changes in soil water content near the ground surface were more noticeable. The
726 DFA based regression model developed is limited in its prediction ability to the range of canal elevations
727 and net recharge by which it was developed. The uncertainty in predictions could be minimized by
728 continuously updating the regression coefficients and constant level parameters as more data on response
729 and explanatory variables are collected. The results of the regression model could be further evaluated
730 using physically based modeling approaches. The approach used in this study could be applied to any
731 system in which detailed physical modeling would be limited by inadequate information on parameters or
732 processes governing the physical system.

733 **Acknowledgements**

734 The authors would like to thank the South Florida Water Management District for providing the funding
735 for this study, the University of Florida IFAS Tropical Research and Education Center, and the University
736 of Florida Agricultural and Biological Engineering Department, Mr. Vito Strano and Mr. Sam Accursio
737 for allowing us to use their lands and Mrs. Tina Dispenza for her contribution towards data collection and
738 processing. We also like to thank the three anonymous reviewers whose comments and suggestions
739 greatly improved this manuscript.

740

741 **References**

- 742 Akaike, H., 1974. A new look at the statistical model identification. *IEEE Trans. Automat. Control* 19,
743 716–723.
- 744 ASCE, 2005., The ASCE Standardized Reference evapotranspiration Equation. Task Committee on
745 Standardization of Calculation of Reference ET. Environment and Water Resources Institute of
746 ASCE. 200 p.
- 747 Allen, R., 2011. REF-ET: Reference Evapotranspiration Calculation Software. User Manual.
- 748 Barquin, L.P., Migliaccio, K.W., Muñoz-Carpena, R., Schaffer, B., Crane, J.H., Li, Y.C., 2011. Shallow
749 Water Table Contribution to Soil-Water Retention in Capillary Fringe of a Very Gravelly Loam
750 Soil of South Florida. *Vadose Zone J*, 10:1–8.
- 751 Chin, D., 1991. Leakage of clogged channels that partially penetrate surficial aquifers. *ASCE J. Hydraulic*
752 *Engineering*. 117, 467-488.
- 753 Chin, D., 2008. Phenomenological models of hydrologic processes in south Florida. *J. Hydrol.* 349, 230–
754 243.
- 755 Dean, T.J., Bell J.P. Baty A.J.B., 1987. Soil moisture measurement by an improved capacitance
756 technique. Part 1: sensor design and performance. *Journal of Hydrology* 93:67.
- 757 Dempster, A.P., Laird, N.M., Rubin, D.B., 1977. Maximum likelihood from incomplete data via the EM
758 algorithm. *J.R. Stat. Soc. Ser. B* 39, 1–38.
- 759 Duwig, C., Normand, B., Vauclin, M., Vachaud, G., Green, S.R., Becquer, T., 2003. Evaluation of the
760 WAVE model for predicting nitrate leaching for two contrasted soil and climate conditions. *Vadose*
761 *Zone J.* 2, 76–89.
- 762 Gabriel, J. L., Lizaso J.I., Miguel, Q., 2010. Laboratory versus Field Calibration of Capacitance Probes.
763 *Soil Sci Soc Am J.* 74, 593-601.

- 764 Genereux, D., Slater, E., 1999. Water exchange between canals and surrounding aquifer and wetlands in
765 the Southern Everglades, USA. *Journal of Hydrology* 219 (1999), 153–168.
- 766 Geweke, J.F., 1977. The dynamic factor analysis of economic time series models. In: Aigner, D.J.,
767 Goldberger, A.S. (Eds.), *Latent Variables in Socio-economic Models*. North-Holland, Amsterdam,
768 pp. 365–382.
- 769 Harvey, A.C., 1989. *Forecasting, structural time series models and the Kalman filter*. Cambridge Univ.
770 Press, New York.
- 771 Kaplan, D., Muñoz-Carpena, R., Wan, Y., Hedgepeth, M., Zheng, F., Roberts, R., Rossmanith, R., 2010a.
772 Linking river, floodplain, and vadose zone hydrology to improve restoration of a coastal river
773 impacted by saltwater intrusion. *J. Environ. Quality* 39 (5), 1570–1584. doi:10.2134/jeq2009.0375.
- 774 Kaplan, D., Muñoz-Carpena, R., Ritter, A., 2010b. Untangling complex groundwater dynamics in the
775 floodplain wetlands of a southeastern U.S. coastal river. *Water Resour. Res.* 46, W08528-10.
776 doi:10.1029/2009WR009038.
- 777 Kaplan, D., Muñoz-Carpena R., 2011. Complementary effects of surface water and groundwater on soil
778 moisture dynamics in a degraded coastal floodplain forest. *J. of Hydrol.* 398, 221–234.
- 779 Lütkepohl, H., 1991. *Introduction to multiple time series analysis*. Springer- Verlag, Berlin.
- 780 Márkus, L., Berke, O., Kovács, J., Urfer, W., 1999. Spatial prediction of the intensity of latent effects
781 governing hydrogeological phenomena. *Environmetrics*. 10, 633-654.
- 782 McDonald, M.G., Harbaugh, A.W., 1988. A modular three-dimensional finite-difference ground-water
783 flow model. *Techniques of Water Resources Investigations of the United States Geological Survey*,
784 Book 6, Chapter A1, US Geological Survey, Reston, Virginia.
- 785 Merritt, M.L., 1996. Simulation of the water table altitude in the Biscayne aquifer, Southern Dade
786 County, Florida, water years 1945-89. *Water-Supply Paper 2458*, US Geological Survey.

- 787 Muñoz-Carpena, R., Ritter, A., Li, Y.C., 2005. Dynamic factor analysis of groundwater quality trends in
788 an agricultural area adjacent to Everglades National Park. *J. Contam. Hydrol.* 80, 49–70.
- 789 Muñoz-Carpena, R., Ritter, A., Bosch, D.D., Schaffer, B., Potter, T.L., 2008. Summer cover crop impacts
790 on soil percolation and nitrogen leaching from a winter corn field. *J. Agricultural Water*
791 *Management.* 95, 633–644.
- 792 Munsell Soil Color Charts., 2000. Revised Edition. Greta G. Macbeth. New Windsor, NY.
- 793 Nash, J.E., Sutcliffe, J.V., 1970. River flow forecasting through conceptual models: Part 1-A. Discussion
794 of principles. *J. Hydrol.* 10, 282–290.
- 795 Nobel, C.V., Drew, R.R.W., Slabaugh, J.D., 1996. Soil survey of Dade County Area, Florida, U.S.
796 Department of Agriculture, NRCS Report, Washington, DC.
- 797 Pathak, S. C., 2008. South Florida Water Management District. South Florida Environmental Report
798 Volume I. Appendix 2-1. Pg. 64. 3301 Gun Club Road, West Palm Beach, FL. Available online
799 at:[http://my.sfwmd.gov/portal/page/portal/pg_grp_sfwmd_sfer/portlet_sfer/tab2236041/volume1/v](http://my.sfwmd.gov/portal/page/portal/pg_grp_sfwmd_sfer/portlet_sfer/tab2236041/volume1/voll_table_of_contents.html)
800 [oll_table_of_contents.html](http://my.sfwmd.gov/portal/page/portal/pg_grp_sfwmd_sfer/portlet_sfer/tab2236041/volume1/voll_table_of_contents.html).
- 801 Ritter, A., Regalado, C.M., Muñoz Carpena R., 2009. Temporal common trends of topsoil water
802 dynamics in a humid subtropical forest watershed. *Vadose Zone J.* 8(2), 437–449.
- 803 Ritter A., Muñoz-Carpena, R., 2006. Dynamic factor modeling of ground and surface water levels in an
804 agricultural area adjacent to Everglades National Park. *J. Hydrol.* 317, 340-354.
- 805 Salas, J.D., 1993. Analysis and modeling of hydrologic time series. p. 19.1–19.72. In D.R. Maidment
806 (ed.) *Handbook of hydrology.* McGraw-Hill, New York.
- 807 Schaffer, B., 1998. Flooding Responses and Water-use Efficiency of Subtropical and Tropical Fruit Trees
808 in an Environmentally-sensitive Wetland. *Annals of Botany* 81, 475–481. SFWMD, 2011. Past and
809 Projected Trends in Climate and Sea Level for South Florida. Hydrologic and Environmental
810 Systems Modeling. 3301 Gun Club Road West Palm Beach, Florida

- 811 Shumway, R.H., Stoffer D.S., 1982. An approach to time series smoothing and forecasting using the EM
812 algorithm. *J. Time Ser. Anal.* 3, 253–264.
- 813 Šimůnek, J., van Genuchten, M. Th., Šejna, M., 2008. Development and applications of the HYDRUS
814 and STANMOD software packages, and related codes, *Vadose Zone J.* 7 (2), 587-600.
- 815 Skinner, C., Bloetscher, F., Pathak, C.S., 2008. Comparison of NEXRAD and Rain Gauge Precipitation
816 Measurements in South Florida. *J. of Hydrologic Engineering.* 14(3), 248-260.
- 817 U.S. Army Corps of Engineers, and South Florida Water Management District, 2009. Comprehensive
818 Everglades Restoration Plan: C-111 spreader canal western project: Draft integrated project
819 implementation report and environmental impact statement.
- 820 USDA Soil Conservation Service. U.S. Department of Agriculture Handbook 18.
- 821 USDA National Agricultural Statistics Service for Miami-Dade County, Florida 2007. Available at:
822 http://www.agcensus.usda.gov/Publications/2007/Online_Highlights/County_Profiles/Florida/cp12
823 [086.pdf](http://www.agcensus.usda.gov/Publications/2007/Online_Highlights/County_Profiles/Florida/cp12)
- 824 Vanclooster, M., Viaene, P., Diels, J., Christiaens, K., 1995. WAVE: A mathematical model for
825 simulating water and agrochemicals in the soil and vadose environment. Reference and user's
826 manual (release 2.0). Institute for Land and Water Management, Katholieke Universiteit Leuven,
827 Leuven, Belgium.
- 828 Water Resources Development Act, 2000. PUBLIC LAW 106–541—DEC. 11, 2000.
829 <http://www.fws.gov/habitatconservation/omnibus/wrda2000.pdf> Retrieved July-23-2010.
- 830 Zou, S., Yu, Y., 1999. A dynamic factor model for multivariate water quality time series with trends. *J. of*
831 *Hydrology* 178 (1–4), 381–400.
- 832 Zuur, A.F., Ieno, E.N., Smith, G.M., 2007. *Analysing ecological data.* Springer- Verlag, Berlin.
- 833 Zuur, A.F., Pierce, G.J., 2004. Common trends in Northeast Atlantic squid time series. *J. Sea Res.* 52, 57–
834 72.

- 835 Zuur, A.F., Fryer, R.J., Jolliffe, I.T., Dekker, R., Beukema, J.J., 2003. Estimating common trends in
836 multivariate time series using dynamic factor analysis. *Environmetrics*. 14 (7), 665–685.